

A three-dimensional classification for WN stars

Lindsey F. Smith,¹ Michael M. Shara² and Anthony F. J. Moffat³

¹*School of Physics, University of Sydney, NSW 2006, Australia*

²*Space Telescope Science Institute, 3700 San Martin Drive, Baltimore, MD 21218, USA*

³*Département de Physique, Université de Montreal, CP6128 Succ A, Montreal, Quebec, H3C 3J7, Canada*

Accepted 1996 January 31. Received 1996 January 29; in original form 1995 April 21

ABSTRACT

A three-dimensional classification for WN stars is presented using (1) the He II 5411/He I 5875 ratio as a primary indicator of ionization, (2) FWHM 4686 and EW 5411 as indicators of line width and strength, and (3) an oscillating Pickering decrement as an indicator of the presence of hydrogen. All WN stars in the Galaxy and two-thirds of the LMC stars are classified on the new system. Almost all spectra inspected fall smoothly into categories within which the spectra are very similar. All ionization subclasses show a tight correlation between line strength and width, with stars containing hydrogen at the weak, narrow end, and WN/C stars near the strong, broad end. H^+/He^{++} correlates with strength and width with a cut-off for the presence of hydrogen, which is slightly dependent on ionization subclass, at about $\text{FWHM } 4686 = 30 \text{ \AA}$ and $\text{EW } 5411 = 25 \text{ \AA}$. The correlations found indicate that high (initial) mass stars evolve as narrow-line stars from late to early ionization subclass. Lower (initial) mass stars evolve with increasing line strength and width, probably to earlier ionization subclass. The He II 4686/N V, III 4604–40 ratio shows a clear correlation with Galactocentric radius, presumably an effect of the Z gradient. C IV 5808/He II 5411 shows no such correlation. LMC WN stars can be classified without difficulty by the criteria established for Galactic WN stars. While individual spectra of a given subtype are similar in the two galaxies, the frequency distributions over ionization subclass, over EW and FWHM in subclasses WN4 and WN5, and hydrogen content in subclasses WN6–8 are different. The effects are presumably due to metallicity, but the causal connection is unclear.

Key words: stars: Wolf–Rayet – Galaxy: stellar content – Magellanic Clouds.

1 INTRODUCTION

Classification of WR stars was first defined by Beals (1938). Modifications to that system by Hiltner & Schild (1966, hereafter HS66) and by Smith (1968a) are in use to this time. These systems were designed for photographic spectra. Lines to be compared were preferably close in wavelength, and line ratios were approximate or only qualitative (e.g., ‘N IV dominates’).

The advent of linear detectors has made it easy to measure ratios of line strength even when the lines are well separated in wavelength. Peak flux measured in units of the continuum, rather than absolute flux, is still necessary to compensate for interstellar reddening if the lines are not adjacent in wavelength.

The WC classification was quantified by Smith, Shara & Moffat (1990b) and needed no modification. The line ratios

already in use define a one-parameter family with the subclasses well separated.

The definition of WN subtypes has never been satisfactory, resulting in a large number of stars that were ‘peculiar’ in some way (see, e.g., Conti, Leep & Perry 1983, hereafter CLP). The Beals and Smith systems were one-dimensional, defining an ionization sequence only. The Hiltner & Schild system added a second dimension, dividing the spectra into narrow-weak-line (A) and broad-strong-line (B) stars. In the new classification system presented here, we add a third dimension – the hydrogen abundance, and refine the definition of the two existing dimensions. Some philosophical considerations are discussed by Smith, Shara & Moffat (1995).

New observations are presented in Section 2. The three-dimensional system is presented in Sections 3 and 4, with classifications for Galactic and LMC WN stars in Section 5.

The system allows simple (and usually) unequivocal classification with line-strength ratios that are easily measured (with a ruler or by eye) from modern digital spectra. It succeeds in sorting the spectra into groups which are nearly identical in appearance. We find that stars exist with almost every possible combination of ionization subclass, narrow/broad and hydrogen/no hydrogen. However, there are also extremely systematic trends of line width, strength, H^+/He^{++} ratio and ionization, which are presented in Sections 6 and 7. Sources of confusion in the old system are discussed in Section 8. Stars which are probably variable are noted in Section 9. Evolutionary implications are discussed in Section 10.

2 NEW OBSERVATIONS

Spectra of 29 Galactic WN and six LMC WN stars were obtained with the '2D-Fruti' spectrograph of the 1-m Yale telescope of the CTIO in 1988 March. The resolution is 4.3 Å. Details are given in Smith et al. (1990b), where we considered the WC stars.

Emission-line strengths are given in Tables 1 and 2 in three ways: equivalent width (EW), total flux (in $\text{erg cm}^{-2} \text{s}^{-1}$) integrated over the line, and peak flux (line only) in units of the continuum. Each has advantages in some situations: EW is traditional; flux is more accurate when lines are strong or when the continuum is underexposed; peak flux is easy to measure on a modern spectrogram and is less sensitive to blending. Accuracy, judged by agreement with other

observers is about 0.1 dex for EW (see Section 9 for details). For strong, well-resolved lines, the FWHM is also given. This is the actual width at half-maximum of the observed profile – not a value from a Gaussian fit (as is common in the literature).

Line ratios of interest are given in Table 3 along with the new classifications. The line strength measure used is (peak line/continuum). The ratio of N IV 4057 to the blend at 4604–40 Å uses whichever of N V 4604 and N III 4640 is the stronger: N V 4604 for WN2–5; N III 4640 for WN5–9 (WN5 is the transition point, and either component can be stronger). The numbers given for H^+/He^{++} are the mean of values derived from the (H + He) 4861 and 4340 lines. They are number ratios derived as the ratio of the (H + He) line to the geometric mean of adjacent He-only lines, minus 1. The factor 0.94 (see Section 3.3 below) is neglected, and no correction is made for optical depth. Negative numbers, of course, have no meaning. We leave them, as calculated, to emphasize the (in)accuracy of the method. Values as negative as –0.3 occur. Comparison with spectra of Torres-Dodgen & Massey (1988, hereafter TM88) or Crowther (1993 and private communication) suggest that this is observational scatter; it corresponds to the usual estimate of $\sigma=0.1$ dex in EW.

3 THE NEW WN CLASSIFICATION

The new classification criteria are specified in Tables 4(a)–(d), and illustrated and described in detail below. Table 4(e)

Table 1. Line strengths for classification lines in WN stars.

Star	HeII 6560				HeI 5875				CIV 5808				HeII 5411				HeII 4861			
WR#	log EW	-log(Ftot)	peak/ctm		log EW	-log(Ftot)	peak/ctm	FWHM	log EW	-log(Ftot)	peak/ctm	FWHM	log EW	-log(Ftot)	peak/ctm	FWHM	log EW	-log(Ftot)	peak/ctm	FWHM
	[A]	[1]	[2]		[A]	[1]	[2]	[A]	[A]	[1]	[2]	[A]	[A]	[1]	[2]	[A]	[A]	[1]	[2]	[A]
6	2.43	9.08	4.77		1.36 P	10.02	0.52	51	1.70	9.68	1.06	55	1.93	9.37	2.32	37	1.79	9.41	1.85	33
7	2.42	10.65	6.23		1.28	11.84	0.39	47	1.85	11.29	1.44	46	1.92	11.19	2.59	31	1.76	11.39	1.85	28
10	1.90	10.80	2.44		0.94 :	11.91	0.17	50	0.86	12.00	0.22	30	0.91	11.93	0.43	17	0.98	11.83	0.51	15
12	2.37 P	10.76	5.70		1.53 P	11.35	1.64	22	0.08 P	12.78	0.14	9 :	1.06 P	11.79	0.69	16	1.46 P	11.41	1.39	20
16	1.99 :	10.08	4.29		1.48 P	10.73	2.27	13	0.72 P	11.50	0.18	46	0.75 P	11.47	0.48	11	1.41	10.78	1.81	13
20	2.08 :	11.96	3.92		1.34	12.83	0.61	38	1.63	12.53	1.35	34	1.59	12.62	1.41	26	1.41	12.92	1.44	16
28		0.85 :	12.70	0.19	...	0.79 P	12.77	0.32	21	1.04	12.56	0.62	16	1.15	12.52	0.83	14
29		0.62	12.80	0.19	22	0.28 P	13.14	0.10	20	0.61 P	12.84	0.19	19	0.80	12.72	0.26	24
31	1.28 :	11.52	0.75		noise	noise	1.08	11.65	0.41	32	0.92	11.78	0.33	...
34		1.04 P	13.19	0.41	33	1.61 P	12.64	1.29	28	1.58	12.70	1.54	24	1.36 ::	12.99	1.10	21
35		1.00	12.86	0.44	25	1.20 P	12.70	0.54	22	1.30	12.66	1.07	17	1.38	12.66	1.33	17
36	1.84 :	12.45	2.68		1.82	12.26	1.18	57	1.58	12.50	1.00	57	1.81	12.27	1.45	47	1.62	12.56	1.12	39
43		0.28	12.93	0.08	26	0.53 P	12.68	0.18	23	0.48	12.78	0.13	27	0.75	12.58	0.19	45
44	1.79	12.08	2.84		0.99	12.68	0.20	56	1.45	12.23	0.68	41	1.57	12.08	1.36	27	1.45	12.17	0.94	28
46	1.75 ::	11.10	1.59		pres?	1.18	11.63	0.57	20	1.04	11.70	0.52	21
49		0.80 P	13.01	0.27	20 :	1.11 P	12.71	0.48	24	1.40	12.44	0.95	24	1.38	12.43	1.04	20
51	1.86 :	12.45	4.00		1.04	13.16	0.37	48	1.41	12.86	1.05	25	1.36	13.05	1.02	21
55		1.56 P	11.12	1.47	20	1.09	11.58	0.67	19	1.41	11.29	1.51	17	1.32	11.44	1.20	15
61	1.79 :	11.45	1.89		0.89	12.62	0.31	27	1.52	12.00	1.11	33	1.56	11.97	1.53	23	1.45	12.05	1.20	21
62	2.01	11.58	2.28		1.64	12.27	0.93	57	1.36	12.57	0.67	38	1.74	12.35	1.60	33	1.46	12.95	0.96	29
63		1.18 P	12.20	0.59	22	0.81 P	12.57	0.30	28	1.08	12.42	0.61	18	0.77	12.99	0.33	19
67	1.72 :	11.37	2.08		1.11 P	12.08	0.62	24	1.30 P	11.90	0.63	31	1.48	11.78	1.36	22	1.28	12.05	0.99	18
71	1.78	10.88	2.09		1.11 P	11.56	0.48	33	1.26 P	11.43	0.66	30	1.56	11.08	1.71	20	1.48	11.06	1.32	21
74	1.58 :P	11.94	1.64		1.58 P	12.40	1.17	25	1.11 P	12.75	0.45	24 :	1.32 P	12.69	1.07	18	1.08 P	13.15	0.76	16
84	1.81 :	11.70	2.67		1.43 P	12.22	0.97	29	1.23 P	12.43	0.60	27	1.46	12.31	1.36	19	1.40 P	12.56	1.32	17
91	1.87	12.24	2.21		1.76 P	12.67	1.48	46	1.26 P	13.21	0.56	35 :	1.51 P	13.15	1.15	27	1.40 P	13.64	1.18	25
108	1.61	10.36	1.49		0.80 P	11.51	0.41	16	0.18 P	12.15	0.07	14	0.68	11.86	0.29	16
110	2.18 :	10.20	2.67		1.79	10.64	0.80	95 :	1.53 P	10.90	0.68	60	1.87 P	10.62	1.32	55	1.75 P	10.86	1.11	52
115	1.57 :	11.26	1.73		1.15 P	11.88	0.61	25	1.11 P	11.96	0.50	27	1.32 P	11.86	1.02	19	1.18	12.19	0.76	18
Br13	2.17	11.77	7.62		1.57 P	12.25	2.00	18	0.86 :	12.94	0.36	28	1.18 P	12.51	0.95	14	1.61	11.92	2.26	16
Br14	1.58	12.71	1.83		noise	48	1.32	13.06	0.75	23	1.52	12.77	1.26	24	1.36	12.73	1.00	19
Br24		0.94 P	13.03	0.48	21	1.08 :P	12.88	0.36	...	1.26 P	12.61	0.92	16	1.40	12.29	1.47	15
Br26		0.92 P	12.85	0.25	30	1.40	12.27	1.10	20	1.43	12.05	1.05	20
Br89	neb ?		noise	39 :	noise	36 :	1.15	12.03	0.68	21	1.43	11.57	1.16	18
Br90	neb		neb	17	0.68 :P	12.79	0.20	36	1.18	12.23	0.65	19	neb

Table 1 — continued

Star WR#	Hell 4686				N III 4640 (see footnote 3)...				N V 4604 (see footnote 4)...				Hell 4541				Hell 4471			
	log EW	-log(Ftot)	peak/ctm	FWHM	log EW	-log(Ftot)	peak/ctm		log EW	-log(Ftot)	peak/ctm		log EW	-log(Ftot)	peak/ctm		log EW	-log(Ftot)	peak/ctm	
	[A]	[1]	[2]	[A]	[A]	[1]	[2]		[A]	[1]	[2]		[A]	[1]	[2]		[A]	[1]	[2]	
6	2.49	8.68	6.54	44		1.83	9.32	1.56		1.58	9.54	1.15		
7	2.63	10.52	11.48	32		1.95	11.20	2.45		1.63	11.52	1.39		0.57	12.56	0.10	
10	1.73	11.06	2.42	20	0.71	12.08	0.20		0.18 P	12.61	0.19		0.60	12.19	0.24		0.20 P	12.58	0.08	
12	1.87	11.03	3.43	18	1.56	11.35	1.56		0.32	12.57	0.20		1.05	11.87	0.50		0.87 P	12.05	0.39	
16	1.65	10.53	2.71	12	1.59 P	10.59	1.93		0.36	11.83	0.21		0.78	11.41	0.38		0.80 P	11.38	0.57	
20	2.35	11.99	8.94	24	1.41	12.96	0.74		1.04 P	13.35	0.72		1.23	13.16	1.04		0.28 P	14.14	0.12	
28	1.81	11.91	3.26	18	1.26	12.46	0.77		0.20 P	13.52	0.14		0.83	12.91	0.40		0.79 P	13.02	0.15	
29	1.48	12.05	1.49	18	0.99	12.55	0.43		-0.70	14.12	0.01		0.20	13.33	0.09		-0.22 P	13.80	0.04	
31	1.81	10.88	2.17	28		0.86 P	11.82	0.29		0.57	12.10	0.17		
34	2.30	12.08	7.72	24	1.32	13.08	0.76		0.93	13.46	0.78		1.34	13.07	0.96		
35	1.99	12.08	5.08	17	1.51	12.57	1.33		0.34	13.74	0.27		1.04	13.06	0.62		0.20 P	14.93	1.50	
36	2.60	11.60	8.33	47		1.72	12.51	1.13		1.62	12.63	1.04		0.68	13.57	0.13	
43	1.20	12.13	0.53	26	0.64	12.70	0.18		-0.15	13.53	0.06		
44	2.35	11.27	7.43	28		1.56	12.08	1.06		1.32	12.28	0.74		
46	2.07	10.66	2.80	36		1.80	10.90	1.55		0.78	11.91	0.32		
49	2.06	11.75	4.78	22	1.20	12.59	0.52		0.78 P	13.01	0.64		0.97	12.84	0.52		
51	2.12	12.31	5.09	25		1.40	13.05	1.02		1.08	13.41	0.47		0.32	14.17	0.16	
55	2.11	10.66	6.34	17	1.86	10.91	2.90		0.63	12.14	0.42		1.34	11.44	1.04		0.81 P	11.96	0.39	
61	2.26	11.24	5.88	27	1.58	11.92	1.10		1.04 P	12.44	1.02		1.30	12.16	0.92		0.61	12.86	0.12	
62	2.47	12.06	8.00	34	2.00	12.59	3.10		1.20 ::	13.41	1.13		1.71	12.95	1.22		0.54 P	13.20	0.17	
63	1.72	12.11	2.60	18	1.54	12.33	1.35		0.46 P	13.42	0.18		1.08	12.86	0.59		0.83 P	13.14	0.22	
67	2.04	11.29	4.56	22	1.76	11.58	1.94		0.79 P	12.56	0.54		1.36	11.98	0.89		0.73 P	12.63	0.21	
71	2.21	10.31	6.51	24	1.89	10.63	2.50		0.98	11.53	0.69		1.41	11.08	1.07		0.78 P	11.71	0.18	
74	1.88	12.43	3.80	17	1.76	12.57	2.26		0.65	13.68	0.45		1.23	13.13	0.83		0.73 P	13.66	0.25	
84	2.11	11.90	6.31	18	1.91	12.12	3.26		0.79	13.25	0.53		1.36	12.70	1.00		0.98 P	13.11	0.31	
91	2.25	12.88	5.15	32	2.01 P	13.15	2.81		...	P Cyg absn on 4640!			1.30 :	13.87	1.07		1.08 P	14.18	0.25	
108	1.04	11.54	0.80	11	1.26	11.33	0.77		0.18 P	12.42	0.12		0.15	12.44	0.10		0.40 P	12.21	0.17	
110	2.64	9.98	6.97	59		2.06	10.60	2.88		1.83	10.86	1.33		0.64 P	12.05	0.22	
115	1.92	11.50	4.07	19	1.54	11.90	1.51		0.49	12.96	0.32		1.20	12.28	0.73		pres P	
Br13	1.94	11.54	5.25	14	1.62	11.85	1.80		-0.30	13.82	0.07		0.90	12.55	0.52		0.76 P	12.68	0.51	
Br14	2.21	11.83	5.76	25		1.45	12.58	1.00		1.18	12.83	0.67		
Br24	1.88	11.76	4.52	15	1.32 P	12.30	1.07		...	P Cyg absn on 4640!			0.79	12.82	0.37		0.15 P	13.44	0.00	
Br26	2.06	11.38	5.07	20	1.18	12.23	0.67		0.04 P	13.38	0.11		0.95	12.44	0.50		0.40 P	12.99	0.00	
Br89	1.96	10.99	4.33	19	1.11 P	11.82	0.56		...	P Cyg absn on 4640!			0.30 :	12.66	0.33		-0.10 P	12.99	0.00	
Br90	1.87	11.34	3.57	18	1.04 P	12.17	0.52		-0.52 P	13.66	0.06		0.48	12.72	0.23		

Star WR#	Hell 4340				Hell 4200				N IV 4057			
	log EW	-log(Ftot)	peak/ctm	FWHM	log EW	-log(Ftot)	peak/ctm		log EW	-log(Ftot)	peak/ctm	FWHM
	[A]	[1]	[2]	[A]	[A]	[1]	[2]		[A]	[1]	[2]	[A]
6	1.40	9.68	0.93	1.41	9.65	0.81			1.49	9.56	0.93	...
7	1.48	11.65	1.04	1.41	11.74	0.86			1.11 ::	12.00	0.48	...
10	0.66	12.10	0.28	0.85	11.89	0.16			1.11	11.63	0.86	12
12	1.20	11.73	0.85	0.89	12.05	0.32			1.08	11.86	0.72	14
16	1.15	11.10	0.89	0.63	11.67	0.25			0.65	11.71	0.40	11
20	1.04	13.38	0.59	1.08	13.37	0.71			1.52	12.96	1.94	14
28	0.78	12.99	0.40	0.70	13.09	0.27			0.97	12.86	0.70	11
29	0.08	13.50	0.07	0.00 :	13.56	0.04			0.74	12.89	0.28	13
31	0.58	12.05	0.12	0.65	11.98	0.21			0.71	11.90	0.21	22
34	1.26	13.20	0.89	1.36	13.14	0.86			1.53	13.01	1.90	17
35	1.00	13.14	0.85	0.93	13.24	0.55			1.30	12.93	1.45	12
36	1.43	12.88	0.73	1.40 :	12.83	0.65			1.40 :	12.93	1.12	21 :
43			0.61 :	12.78	0.19	17 :
44	1.04	12.55	0.56	1.11	12.47	0.51			1.18	12.41	0.68	22
46	0.65	11.99	0.16	0.48 ::	12.14	0.18			0.30 ::	12.26	0.11	...
49	1.15	12.68	0.68	1.00	12.84	0.50			1.43	12.41	1.52	15
51	0.81	13.71	0.45	0.85	13.70	0.34			1.30	13.30	1.03	17
55	1.05	11.71	0.76	0.85	11.90	0.56			1.32	11.42	1.60	12
61	1.15	12.32	0.64	1.18	12.28	0.66			1.52	11.92	1.90	17
62	1.26	13.53	0.81	1.18	13.67	0.94			1.68	13.25	1.64	...
63	0.68	13.34	0.32	0.85	13.22	0.40			1.13	13.00	0.80	16
67	1.04	12.33	0.62	1.04	12.33	0.51			1.46	11.93	1.79	15
71	1.10	11.35	0.69	1.15	11.25	0.70			1.51	10.86	2.10	15
74	0.58	13.86	0.32	0.86	13.66	0.42			1.32	13.29	1.46	13
84	1.04	13.08	0.72	1.15	13.01	0.74			1.46	12.76	1.93	14
91	1.20 :	14.15	0.79	1.58 :	13.92	0.78			1.79 :	13.82	1.91	29
108	0.45 :	12.16	0.16	0.45 :	12.17	0.10			0.11	12.51	0.11	...
110	1.45	11.23	0.63	1.54	11.16	0.76			1.82	10.88	1.57	...
115	0.93	12.64	0.46	1.06	12.54	0.57			1.26	12.40	1.26	14
Br13	1.23	12.18	1.06	0.76 P	12.62	0.43			1.08	12.28	0.77	14
Br14	0.90	13.06	0.43	0.97	12.96	0.45			0.83	13.06	0.29	18
Br24	1.04	12.52	0.64	0.66	12.87	0.28			1.08	12.43	0.80	12
Br26	0.95	12.39	0.46	0.82	12.50	0.36			1.11	12.18	0.79	15
Br89	0.94	11.90	0.44	0.71	12.09	0.26			1.04	11.72	0.68	14
Br90	neb	0.43	12.70	0.15			0.89	12.21	0.52	13

- (1) Units of total flux are $\text{erg cm}^{-2} \text{s}^{-1}$ integrated over the line.
(2) peak/ctm is the flux ratio of (peak-line only)/(continuum at that wavelength).
(3) N III 4640 includes N V 4620 in WN5–8 spectra.
(4) N V 4604 includes N V 4620 in WN3–5 spectra.

Table 2. Line strengths for other lines in WN stars.

Star	NV 4944 &/or HeI 4922			HeII, NIII, SiIV 4100			HeI 3888			NIV 3480			log(EW,IS abs'n).....			log(EW,H abs'n)		
WR#	log EW	-log(Ftot)	peak/ctm	log EW	-log(Ftot)	peak/ctm	log EW	-log(Ftot)	peak/ctm	log EW	-log(Ftot)	peak/ctm	FWHM	Nal 5890	4430	Call 3934	H9, 3835	H11,3770
	[A]	[1]	[2]	[A]	[1]	[2]	[A]	[1]	[2]	[A]	[1]	[2]	[A]	[A]	[A]	[A]	[A]	[A]
6	1.18	10.01	0.46	1.71	9.34	1.39	0.97 P	9.99	0.33	2.10	8.68	4.46	24	...	0.30	0.56
7	1.28	11.88	0.37	1.57	11.54	1.03	1.08 :	12.00	0.38	2.21	10.80	6.44	24	0.32	0.60
10	0.11 :	12.71	0.13	1.08	11.65	0.32	1.08	11.49	0.90	12	0.52	...	-0.15	0.04	0.00
12	0.76 P	12.11	0.31	1.51	11.43	1.22	1.10 P	11.86	0.85	0.91 P	11.96	0.59	12	0.23	0.30
16	0.84	11.35	0.47	1.49	10.86	1.29	1.02 P	11.44	1.03	pres??	0.30
20	1.00	13.28	0.33	1.52	12.96	1.33	0.86 P	13.66	0.50	1.73 :	12.92	3.42	17	0.36	0.70
28	1.26	12.56	0.62	0.48 P	13.36	0.08	pres	0.30	0.70	0.08
29	0.00	13.51	0.07	0.75	12.84	0.19	0.15 P	13.51	0.06	0.30	13.44	0.14	15	0.08	0.78	0.00	-0.15	0.30
31	0.38	12.34	0.16	0.67	11.96	0.15	noise	1.28	11.40	0.93	16	...	0.70	...	0.45 ::	...
34	1.59	12.93	1.44	0.94	13.62	0.47	1.74	12.86	3.23	16	...	0.70
35	1.52	12.69	1.29	0.89 P	13.40	0.44	pres	0.38	0.30	0.28
36	1.20 3)	12.96	0.37	1.77 :	12.54	1.36	1.38	13.02	0.68	1.90 :	12.5:	2.70	29	0.15	0.60
43	0.18	13.14	0.06	0.15 a	pres	0.11	0.70	-0.22	-0.07	...
44	0.98	12.65	0.32	1.32	12.27	0.68	1.77	11.84	2.78	17	0.18	0.70	0.62
46 4)	1.18	11.56	0.63	0.60 :	11.97	0.22	0.48 ::	11.96	0.20	...	0.59	0.30	-0.10
49	0.66	13.14	0.21	1.45	12.39	1.05	1.45	12.51	2.06	13	0.18	0.70	0.30
51	0.81	13.56	0.34	1.32	13.25	0.74	pres	13.35	...	14	...	0.78
55	0.89	11.86	0.34	1.66	11.07	1.78	0.97 P	11.77	0.59	1.21 P	11.61	1.37	11	...	0.70
61	0.92	12.59	0.33	1.61	11.82	1.56	0.74 P	12.68	0.20	1.74 :	11.64	3.33	16	0.15	0.30	0.48
62	1.11	13.28	0.43	1.78	13.10	2.00	pres	pres?	0.18
63	1.36	12.74	0.86	0.86 P	13.37	0.29	1.15 :P	13.28	0.96	19	0.48	0.76	...	0.41	...
67	0.81	12.49	0.16	1.64	11.76	1.71	0.63 P	12.80	0.23	1.51	12.08	2.14	14	...	0.60	0.18
71	0.90	11.65	0.38	1.72	10.65	1.83	0.60 P	11.71	0.21	1.52 P	10.75	2.25	12	0.04	0.00	0.08
74	0.57 :	13.64	0.23	1.51	13.07	1.30	pres,P	noise	13.68	...	10	0.49	0.60
84	1.03	12.90	0.32	1.70	12.51	1.98	0.83 P	13.48	0.45	1.34 :	13.24	1.74	10	pres?	0.60
91	1.30	13.71	0.74	1.89 :	13.68	2.77	pres?P	pres	0.28	0.78	0.38
108	1.00 :P	11.61	0.43	pres?	0.43	0.00
110	1.26	11.33	0.45	2.12	10.59	2.39	1.18 P	11.53	0.29	1.96 P	10.93	3.00	29	0.15	0.30	-0.10
115	0.53	12.80	0.19	1.46	12.18	1.22	0.64 P	13.08	0.22	pres	0.30
Br13	0.82	12.72	0.39	1.46	11.88	1.20	1.00 P	12.31	0.83	0.96 :	12.34	0.43	16::	...	0.30	-0.10
Br14	0.72	13.40	0.28	1.08	12.82	0.52	1.81 :	12.06	2.88	18	0.34	0.30	0.00
Br24	1.28	12.23	0.91	0.56 P	12.94	0.24	0.64	12.77	0.37	11	...	0.00	...	-0.05	...
Br26	0.49	13.03	0.13	1.30	11.99	0.86	0.58 P	12.68	0.24	1.11	12.12	0.74	16	...	0.00	...	-0.15	...
Br89	1.23	11.56	0.65	0.56	12.15	0.24	0.90	11.71	0.33	17	0.18	0.48
Br90	nebl	1.18 ::	11.94	0.44	0.52	12.58	0.19	0.77	12.29	0.29	25	...	0.48	-0.22

(1) Units of total flux are $\text{erg cm}^{-2} \text{s}^{-1}$ integrated over the line.

(2) peak/ctm is the flux ratio of (peak-line only)/(continuum at that wavelength).

(3) Both 4922 and 4944 are present and blended.

(4) WR 46 has O VI 3611,34 with $\log EW = 0.90$, $-\log(F_{\text{tot}}) = 11.59$ and peak/ctm = 0.38.

gives examples of stars which fall in the mid-range of the classification criteria; so far as is possible, stars in both northern and southern hemispheres are listed.

3.1 Ionization sequence

Spectra of single, narrow-line, Galactic stars, WN4–9 are shown in Fig. 1. We have chosen examples, so far as possible, that are near the extremes of He II/He I ratio for each subclass and are without hydrogen. Unfortunately, we do not have a spectrum of WR 152, the only single, narrow-line WN3 star in the Galaxy; neither do we have a spectrum of WR 107 or 123, the two WN8 stars without hydrogen. No WN9 star is known without hydrogen. This paper does not purport to define the WN9 subclass; see Crowther, Hillier & Smith (1995a). The spectrum of WR 108 is shown in Fig. 1 to facilitate the link to the Crowther et al. system for the WN9–11 stars. Plots are in $2.5 \log F_{\lambda}$ ($\text{erg cm}^{-2} \text{s}^{-1} \text{\AA}^{-1}$) to enhance the visibility of weak lines and preserve the representation of line strength when the continuum flux changes (mostly due to reddening).

The ionization sequence is defined and enumerated (see Table 4a) by ratios of peak line flux measured in units of the

local continuum. This choice is made because (1) it corresponds to the visual impression, (2) it is easy to measure on a modern digital spectrum, and (3) it is relatively insensitive to blending.

3.1.1 He ratios

The ratio of He II 5411 to He I 5875 is the primary discriminant of ionization subclass. The lines are shaded in Figs 1 and 2 to enhance visibility. Previous systems depended primarily on the nitrogen lines. The helium ratio is chosen for several reasons: (1) the dominant N lines in the visible spectrum are all prone to selective excitation effects (e.g. Conti, Massey & Vreux 1990; Hillier 1987) and sometimes give discordant results; in a nearly pure helium atmosphere, the helium lines should give a more consistent temperature sequence; (2) the two helium lines are used (Schmutz, Hamman & Wessolowski 1989, Hamann, Kosterke & Wessolowski 1993, hereafter HKW, Crowther et al. 1995a, b, c) to derive stellar parameters using model atmospheres; (3) they are uncontaminated; (4) He II 5411 is well isolated in all subclasses, and He I 5875 is relatively isolated; and (5) they are in the yellow–red where interstellar absorp-

Table 3. New data. Line ratios of interest.

Star	New	4686	5411	H+	HeII 5411	NV 4604	NIV 4057	CIV 5808	CIV 5808	NIV3480
WR#	Class	FWHM	E W	He++	HeI 5875	NIII 4640	N 4604-40	HeII 5411	HeI 5875	NIV4057
VdH88	This paper	(A)	(A)	by #			Peak line / continuum ratios			
[1]	[2]	[3]	[4]	[5]	[6]	[7]	[8]	[9]	[10]	[11]
6	WN4b	44	86	0.0	4.5	...	0.6	0.5	2.0	4.8
7	WN4b	32	84	0.0	6.6	...	0.2	0.6	3.7	13.0
10	WN5h(+OB)	20	8.2	0.5	2.5	1.0	4.3	0.5	1.3	1.0
12	WN8h	18	12	1.3	0.4	0.1	0.5	0.2	0.1	0.8
16	WN8h	12	5.6	2.6	0.2	0.1	0.2	0.4	0.1	...
20	WN5o	24	39	-0.1	2.3	1.0	2.6	1.0	2.2	1.8
28	WN6(h)	18	11	0.4	3.3	0.2	0.9	0.5	1.7	...
29	WN7h+abs	18	4.1	0.6	1.0	0.0	0.7	0.5	0.5	0.5
31	WN4o+O8V	28	12	-0.1	0.7	4.4
34	WN5o	24	38	-0.1	3.8	1.0	2.5	0.8	3.1	1.7
35	WN6h	17	20	0.5	2.4	0.2	1.1	0.5	1.2	...
36	WN5b	47	65	-0.1	1.2	...	1.0	0.7	0.8	2.4
43	WN6o(+O5)	26	3	...	1.6	0.3	1.1	1.4	2.3	...
44	WN4o	28	37	-0.1	6.8	...	0.6	0.5	3.4	4.1
46	WN3b pec	36	15	-0.1	0.1	1.8
49	WN5(h)	22	25	0.4	3.5	1.2	2.9	0.5	1.8	1.4
51	WN4o	25	26	0.3	1.0
55	WN7o	17	26	0.0	1.0	0.1	0.6	0.4	0.5	0.9
61	WN5o	27	36	-0.1	4.9	0.9	1.7	0.7	3.6	1.8
62	WN6b	34	55	-0.3	1.7	0.4	0.5	0.4	0.7	...
63	WN7o+OB	18	12	-0.4	1.0	0.1	0.6	0.5	0.5	1.2
67	WN6o	22	30	-0.1	2.2	0.3	0.9	0.5	1.0	1.2
71	WN6o	24	36	-0.1	3.6	0.3	0.8	0.4	1.4	1.1
74	WN7o	17	21	-0.3	0.9	0.2	0.6	0.4	0.4	...
84	WN7o	18	29	0.0	1.4	0.2	0.6	0.4	0.6	0.9
91	WN7b	32	32	0.0	0.8	0.0	0.7	0.5	0.4	...
108	WN9h	11	0.2	0.1	...	0.2	...
110	WN5b	59	74	-0.3	1.6	...	0.5	0.5	0.8	1.9
115	WN6o	19	21	-0.2	1.7	0.2	0.8	0.5	0.8	...
Br13	WN8h	14	15	1.7	0.5	0.0	0.4	0.4	0.2	0.6
Br14	WN4o	25	33	-0.1	0.3	0.6	...	9.9
Br24	WN6h	15	18	1.3	1.9	...	0.7	0.4	0.8	0.5
Br26	WN6(h)+abs?	20	25	0.3	4.4	0.2	1.2	0.9
Br89	WN6h	19	14	1.0	1.2	0.5
Br90	WN6(h)	18	15	0.1	1.0	0.3	...	0.6

tion is lower – an advantage as we push to fainter and more reddened stars.

When the He II 5411 peak/continuum ratio drops below 0.2, classification by helium alone fails. Where He I is strong, the stars are WN9–11, and the classification of Crowther et al. (1995a) takes over smoothly. When both He II and He I are weak, absorption lines are always present and there are two possibilities: either the star is a binary or it is an ‘abs’ star; see below under ‘absorption lines’. Fig. 3 shows the relationship between ratios of peak line flux/continuum and EW. EW data are taken from the sources quoted in Table 6 (see Section 5). The scatter is considerable, probably due to the low accuracy of published He I 5875 EWs (see Section 9). The EW ratio is lower by about 0.1 dex due to the greater width of He I 5875. Table 4(a) includes a calibration of the EW ratio for this primary ionization criterion.

3.1.2 Nitrogen ratios

N ratios are also given in Table 4(a), and are qualitatively similar to the old system. Separation of flux due to N V and

N III in the 4604–40 blend is subjective. For WN5–8 spectra, N V 4620 blends with N III 4634,40; what is measured as 4604 is the blue emission bump separated from the blend by the violet absorption component of 4620. However, the ratio of the peak flux at 4640 and 4604 is well defined and easy to measure (or estimate by eye) from the spectra. This ratio is a primary criterion for distinguishing WN4/5/6. Absence of N III, N IV and N V still defines WN2. Near-vanishing N IV helps define WN3, but is often hard to apply in practice; disappearance of C IV 5808 between WN4 and WN3 is a more practical discriminant (see Section 3.1.3).

WN5 is a curious, but very uniform subclass – at least for the narrow-line spectra. The He II/He I ratios overlap both WN4 and WN6. The spectra are distinguished by N V ~ N III in the 4604–4640 blend. Because this can be difficult to assess at low resolution, we also require N IV 4057 or C IV 5808 to be strong. Both lines peak, relative to N III and He II, respectively, at WN5; their synchronous behaviour is consistent with a similar ionization potential. WN5 and WN6 are hard to separate when the lines are broad; this is discussed later (Section 4), after the systematic behaviour of subclass properties has been described.

3.1.3 C iv/He ratios

He I 5875 is vanishingly weak in WN4 and totally absent in WN3; consequently, the He II/He I ratio does not serve well to discriminate between WN4 and WN3. (The boundary is uncertain but has been set, provisionally, at He II/He I = 10.) WN3 is previously defined by weak N IV relative to N V; N IV

is not easy to observe because of its location in the blue and blending with He II 4026 and He I, He II, Si IV 4100. However, C IV 5808 and He II line strengths increase steadily from WN7 to WN4, and then C IV suddenly disappears at WN3 while He II remains strong; this serves well as a discriminator. Disappearance of C IV 5808 at the same time as N IV 4057 is consistent with C IV having a slightly lower ionization potential than N IV. Note that the strength of C IV is assessed relative to He II, not to the adjacent He I line.

A criterion that uses a ratio of two different elements can be affected by abundance. However, unlike the He II/N V,III ratio (see Section 6.2), neither C IV/He II nor C IV/He I shows a correlation with Galactocentric radius – i.e., there seems to be little correlation with the primordial abundance. This is odd, but useful. The enhancement of C at the end of the WN phase is predicted and observed to occur very suddenly; the C lines are either normal (WN) or very strong (and the classification becomes WN/C; see Section 3.5 below). Confusion from this source is not expected.

The extreme sensitivity of the ratio C IV/He I to ionization makes it a useful indicator for all subclasses, especially in broad-line or binary spectra where other features become difficult to assess.

3.1.4 He/N ratio

The He II 4686/N V,III 4604–40 ratio is not given as a classification indicator. It is found (see Section 6.2) to be sensitive to both ionization and to primordial abundance. In the event of no other information, it could be used by comparison with stars located in regions of similar Z .

3.2 Line width and strength

Fig. 2 shows the broad-line spectra, WN3–7, to be contrasted with Fig. 1, which shows the narrow-line spectra. No broad-line star is known in the WN8 subclass. Figs 4 and 5 show the 4600-Å region for WN4b and WN5–6b, respectively, at higher scale.

Strength and width of lines were incorporated in the classification system of HS66. The importance of this parameter has since been validated: CLP and HKW have noted that strong-line stars rarely show hydrogen; HKW find that strong- and weak-line stars form different sequences in the $T_{\text{eff}} L$ domain. The dividing line used by HKW is $EW\ 5411 = 40\ \text{\AA}$, with strong-line spectra designated ‘s’ and weak-line spectra designated ‘w’.

Strength and width are closely correlated (see Section 7). We use two criteria (Table 4b) for broad-strong-line stars: $FWHM\ 4686 \geq 30\ \text{\AA}$ and/or $EW\ 5411 > 40\ \text{\AA}$ (the HKW criterion). It will be shown that these are essentially equivalent for most single stars. For the line-width criterion, $FWHM\ 4686$ is the obvious choice because of its superior strength. For the line-strength criterion, we choose $EW\ 5411$ rather than $EW\ 4686$ for several reasons: (1) $EW\ 5411$ is used by HKW to separate ‘s’ and ‘w’ stars, and we wish to make clear the relationship between these two criteria; (2) $EW\ 4686$ has been bedevilled in the past with inaccuracies due to saturation, calibration of the density–intensity relation, and difficulty in setting the continuum; $EW\ 5411$ seemed a safer parameter; and (3) appearance of He II 5411 in emission more or less defines the traditional WR phase – as distinct

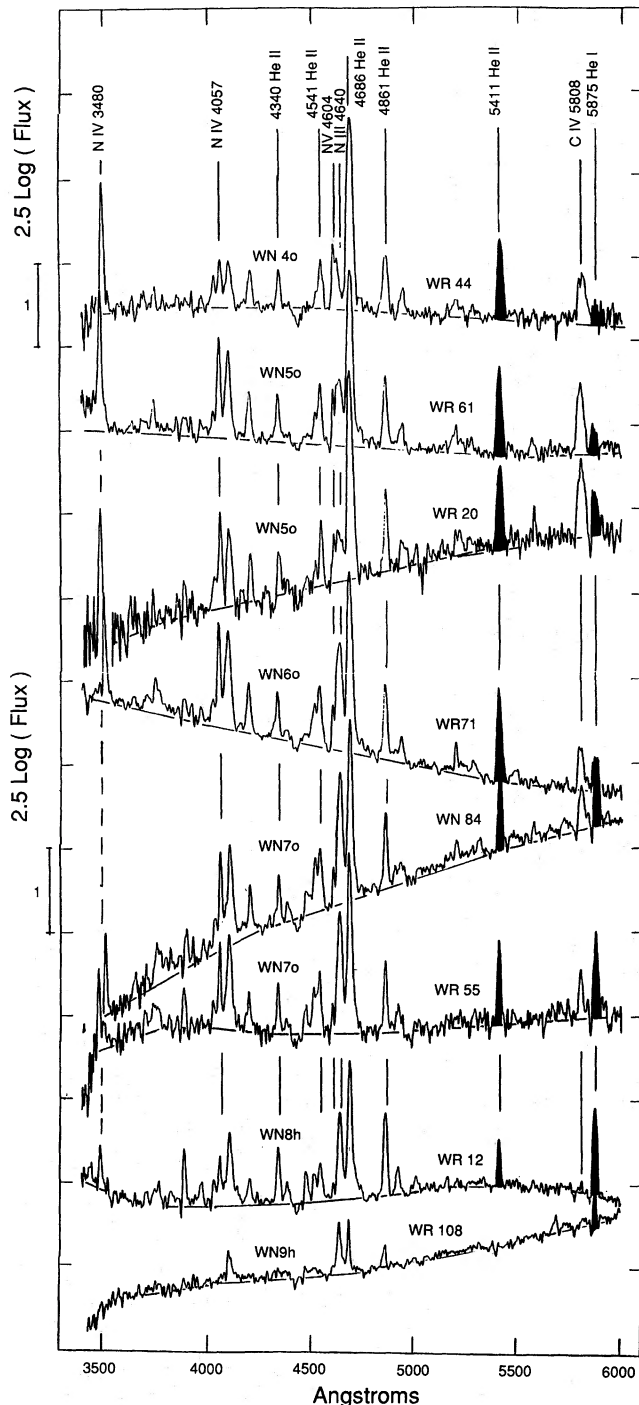


Figure 1. Spectra of single, narrow-line, Galactic stars, WN4–9. We have chosen examples, so far as possible, that are near the extremes of the He II 5411/He I 5875 ratio for each subclass and are without hydrogen. The He II 5411 and He I 5875 lines are shaded to enhance visibility.

Table 4a. The ionization sequence criteria for WN stars.

Ionisation Subclass	<u>HeII 5411</u> HeI 5875			<u>NV 4604</u> NIII 4640			<u>NIV 4057</u> NV,III 4604-40 ¹⁾			<u>CIV 5808</u> HeII 5411			<u>CIV 5808</u> HeI 5875		
	Peak/Continuum			Equivalent Widths			Peak/Continuum			Peak/Continuum			Peak/Continuum		
	bndry	median	bndry	bndry	median	bndry	bndry	median	bndry	bndry	median	bndry	bndry	median	bndry
WN2	No HeI			No HeI			No NV			No CIV			No CIV		
WN3	> 10			> 9			No NIII			< 0.1			< 0.2		
WN4	4 - 8 - 10			3 - 6 - 9			> 2			0.6			0.2 - 0.5 - 0.8		
WN5	1.25 - 4 - 8			1 - 3 - 6			0.5 - 1 - 2			1.25 - 2.5 - or			0.6 - 0.8 - 2.0		
WN6	1.25 - 2 - 4			1 - 2 - 3			0.2 - 0.3 - 0.5			0.8			0.3 - 0.4 - 0.6		
WN7	0.65 - 1 - 1.25			0.5 - 0.75 - 1			0.1 - 0.15 - 0.25			0.6			< 0.5		
WN8	0.1? - 0.4 - 0.65			0.1? - 0.25 - 0.5			0.05 - 0.1? - 0.25			0.2			< 0.4		
WN9	< 0.1?			0			< 0.1?				

When a value is defining, the item is boxed.

(1) The peak of the N v,III 4604-40 blend is taken, regardless of which component dominates.

Table 4b. The strength-width criteria for WN stars.

Designation	Criteria	
	FWHM 4687	EW 5412
b	> 30 Å	and/or > 40 Å

No designation for 'not b'.

Table 4c. The hydrogen criteria for WN stars.

Designation	4861/√(4541*5411) - 1 and/or 4340/√(4200*4541) - 1
o	0
(h)	< 0.5
h	> 0.5

Table 4d. Absorption line criteria for WN stars.

Designation	Criterion
+OB	SB2 or H absorption lines without evidence of H emission.
(+OB)	Visual companion which is usually present on spectra.
+abs	Absorption lines of unknown origin.
ha	Absorption lines from the WR star, H present in emission.

Table 4e. Examples of single stars in each category of the classification system.

Ionisation Subclass	Narrow lined			Broad lined
	h	(h)	o	b
WN2	WR 2
WN3	...	WR 152 #		Br 1
WN4	...	WR 128	WR 44, 129	WR 6, 18
WN5	WR 10*, 109?	WR 49	WR 34	WR 36, 110
WN6	WR 35, 85	WR 28	WR 67, 115	WR 62
WN7	WR 158	WR 82	WR 55, 74	WR 91, 100
WN8	WR 40, 16	WR 66	WR 107, 123	...

#WR 152 has discordant H⁺/He⁺⁺ determinations.

*WR 10 is a visual binary.

?WR 109 may have unusually weak N iv 4057; see comment to Table 6.

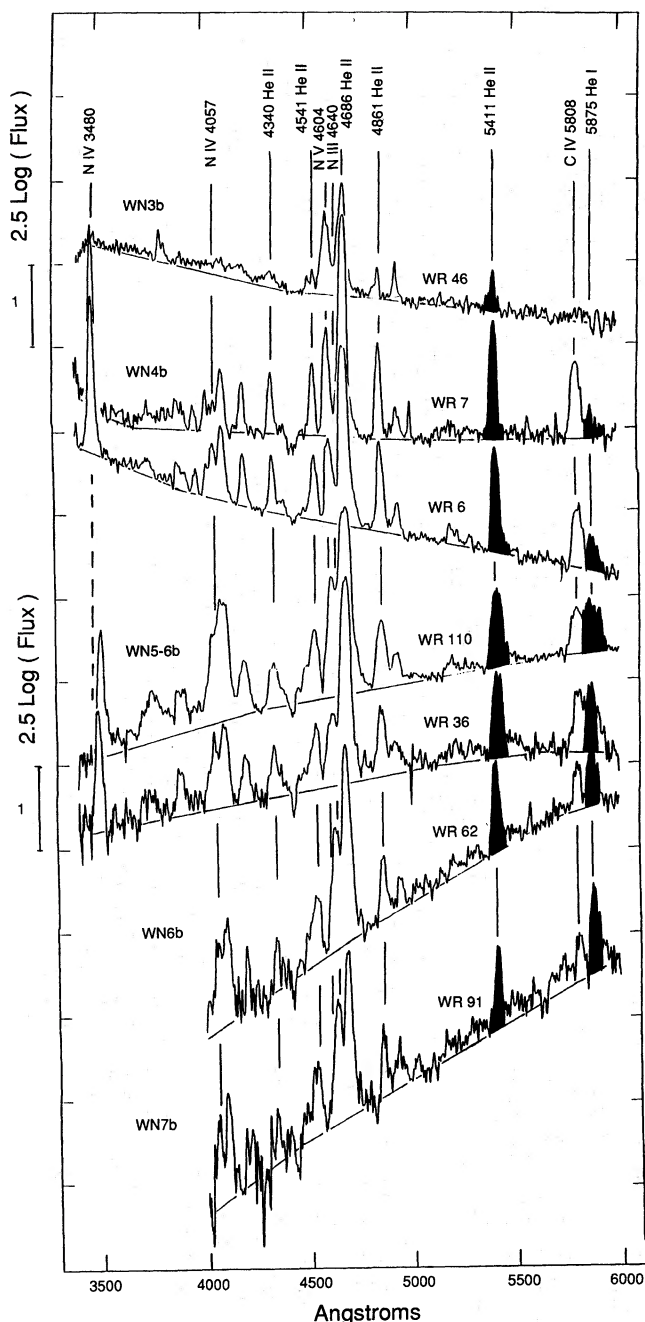


Figure 2. Spectra of single, broad-line, Galactic stars, WN3–7. No broad-line star is known in the WN8 subclass. The He II 5411 and He I 5875 lines are shaded to enhance visibility.

from the transition types WN9–11. When measurement of *EW* 4686 becomes reliable it may prove to be more useful. (*FWHM* 5411 and *FWHM* 4686 are generally the same in the mid-range, 20–50 Å. For *FWHM* 4686 < 20 Å, 5411 is narrower – down to half the width; for *FWHM* 4686 > 50 Å, 5411 is wider by as much as 20 per cent).

The broad-strong-line spectra are designated ‘b’ for ‘broad’. All considerations (see Section 7) indicate that the ‘b’ stars defined here and the ‘s’ stars defined by HKW (and the ‘B’ stars defined, less precisely, by HS66) are identical

groups. However, to avoid confusion in the transition between the use of the various classifications, we assign a unique symbol.

Because superposition of an OB spectrum reduces the *EW* but not the *FWHM* of the lines, we consider *FWHM* 4686 to be the primary discriminator. Because line width is so obvious and easy to measure, no symbol is needed for ‘not b’, reducing the alphabet soup in the classification. Measured line width is affected by spectral resolution, and this is taken into account when assigning ‘b’ type; however, the matter is critical only when the spectrum is composite and the line strength is unknown.

As will be shown (Section 7) the two criteria for b-status are usually fulfilled together. Stars which qualify for b-status on *FWHM*, without passing the *EW* criterion are usually known composites. A few stars with *FWHM* 4686 slightly less than 30 Å qualify for b-status on the *EW* criterion alone (Br 3, 20, 23 and 35 in the LMC).

3.3 Hydrogen

The presence of H is detected by oscillation of the Pickering decrement (PD) caused by coincidence of a H Balmer series line with every second Pickering line. The method was pioneered by Bastor & van Blerkom (1970) and first used systematically by Smith (1973). It is most clearly expounded by CLP. The relationship (Castor & van Blerkom 1970) between line flux and ionic abundance is $F(\text{H} + \text{He})/F(\text{He}) = 0.94 N(\text{H}^+ + \text{He}^{++})/N(\text{He}^{++})$. For classification purposes, hydrogen is detected if the (H + He) lines, 4340 and/or 4861, clearly exceed the height of a line drawn between the peaks of the pure He II lines, 4200, 4541 and 5411. Quantitatively, the relative abundance of $\text{H}^+/\text{He}^{++}$, by number, is determined by the ratio of either of the (H + He) lines to the geometric mean of pure He lines on either side, minus 1 (see Table 4c). If both ratios can be determined, the average has been adopted. Since adjacent Pickering lines have nearly the same width, peak line/continuum or *EW* measures should give the same result.

Figure 6 shows examples of WN5 and 6 stars with no hydrogen, ‘o’, marginal hydrogen, ‘(h)’, and definite hydrogen, ‘h’. The five strong Pickering lines used for $\text{H}^+/\text{He}^{++}$ estimation are shaded, and the peaks of lines with and without hydrogen contribution are joined to enhance the visibility of the criterion used.

Comparison of our spectra with those of TM88 and Crowther (1993 and private communication) indicate (in agreement with HKW) that the reliable detection limit by this method is about $\text{H}^+/\text{He}^{++} = 0.5$ by number. Fortunately, this appears also to be the dividing line where the H presence has a significant effect on derived physical parameters (see HKW). Stars with no detectable H are designated ‘o’. Stars with $\text{H}^+/\text{He}^{++} \geq 0.5$ (clearly present on the PD) are designated ‘h’. Stars with $\text{H}^+/\text{He}^{++}$ between 0 and 0.5, for which hydrogen detection by the PD method is unreliable, are designated ‘(h)’. Since ‘b’ stars rarely have hydrogen, the ‘o’ is subsumed in the ‘b’; i.e., a ‘b’ star has no hydrogen unless specifically indicated otherwise.

The PD method assumes that the atmosphere is optically thin. This is not true for early members of the Pickering series in ‘b’ and ‘s’ stars. However, later members of the Pickering series are optically thin, and no case is known of a

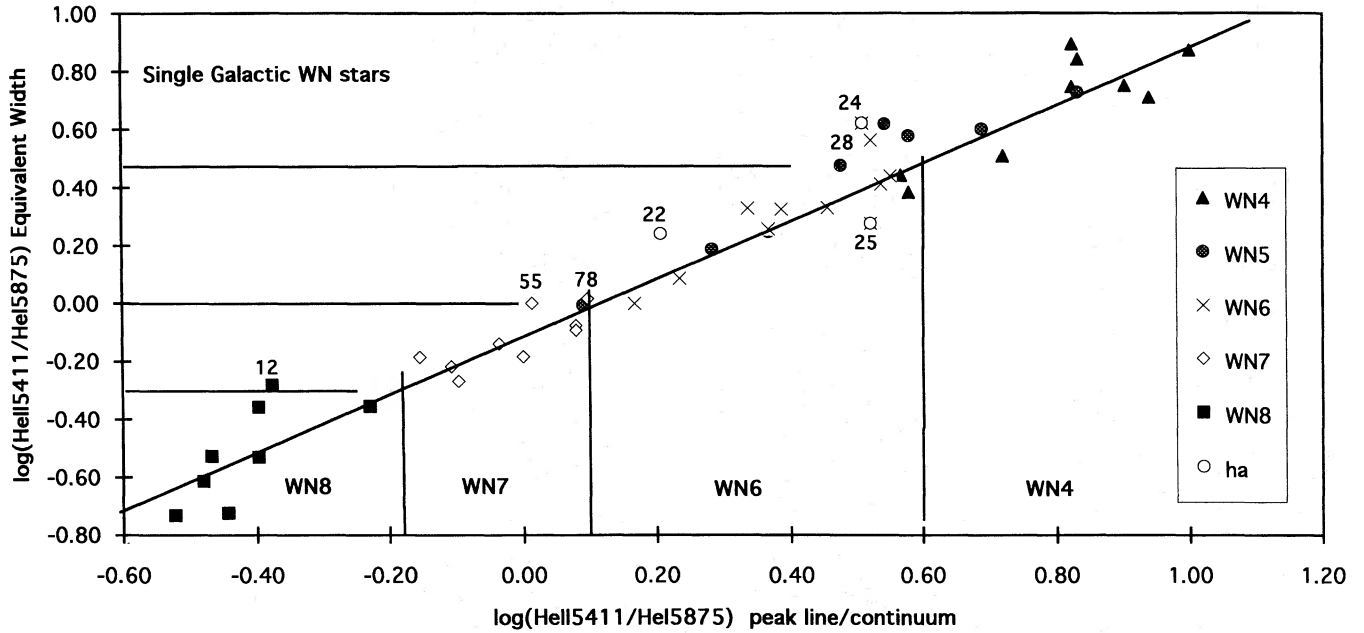


Figure 3. The plot of EW ratios versus peak line/continuum ratios for the primary ionization criterion He II 5411/He I 5875. Boundaries are those specified in Table 4(a).

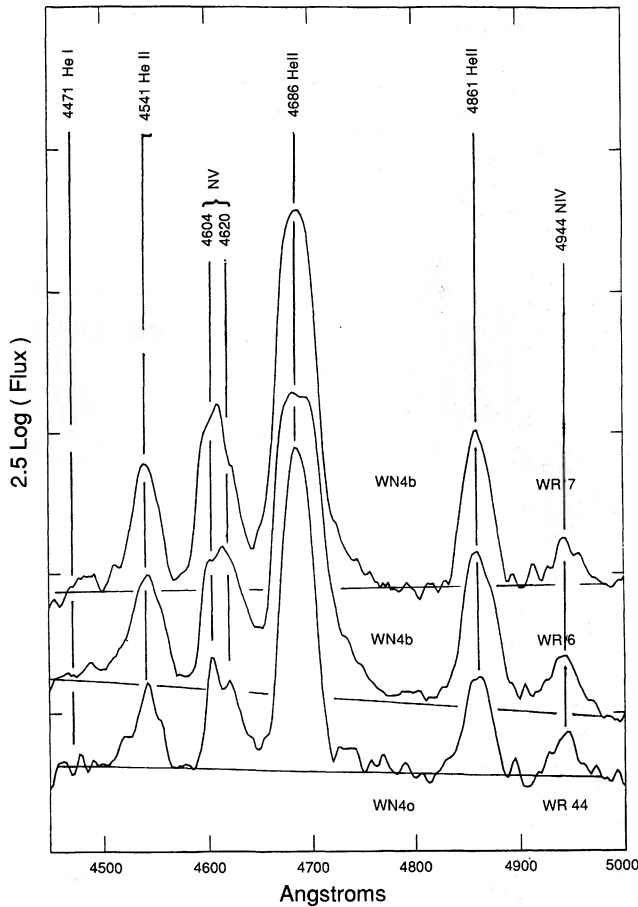


Figure 4. The 4600-Å region for two WN4b stars, WR 6 and 7, and a WN4o star, WR 44, for comparison. The main difference in line width and strength.

b/s star with $H^+/He^{++} > 0.5$; the only b/s stars in which hydrogen has been detected in marginal abundance ($H^+/He^{++} < 0.5$) are WR 136 and Br 54.

Determination of H^+/He^{++} from a composite (+OB) spectrum is very uncertain; the superposed absorption usually affects (H + He) lines more than it affects the pure He lines. The relationship between (H^+/He^{++}) and total H/He will be subclass-dependent, because later subclasses have more He in the singly ionized state.

3.4 Absorption lines

Some spectra with absorption lines are shown in Fig. 7. The Beals definition of a WR spectrum disallowed the presence of absorption lines except for violet-displaced absorption in P Cygni profiles. When absorption lines were present, they were assumed to arise from a companion. Since then, absorption lines have been shown, in some cases, to be intrinsic to the WR star. In those cases, the absorption is violet-displaced (see Crowther et al. 1995a), as was allowed by Beals. However, confusion arises because, when the emission is weak and the dispersion is low, the displacement is not conspicuous. A more consistent classification designation is needed and may, in the future, become a full fourth dimension. For the moment, the situation is still somewhat confused. We suggest the following standardization of usage, summarized in Table 4(d).

Following van der Hucht et al. (1981), '+ abs' has been used to designate spectra with absorption lines where either the absorption lines are established to come from the WR star (and are violet-displaced), or where the origin is (as yet) unknown. We propose to use 'a' for stars in which the absorption comes from the WR, and reserve '+ ab' for the situation where the origin is unknown. (The final classification could be either 'a' or '+ OB', or both.) The '+ OB'

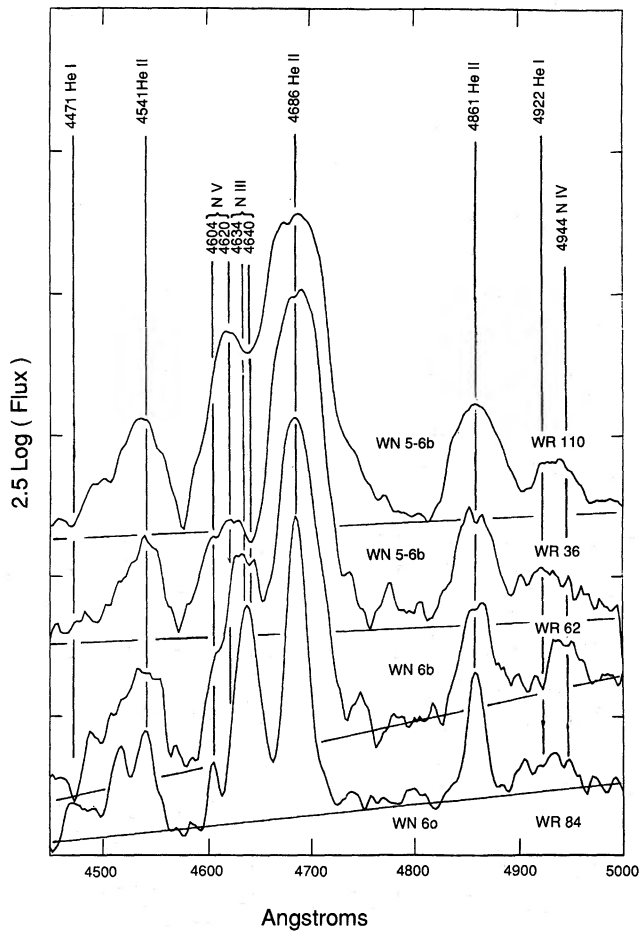


Figure 5. The 4600-Å region for the WN5-6b stars, WR 36 and 110, the WN6b star, WR 62, and a WN6o star, WR 84, for comparison. While the broad-line stars, in every other respect, classify as WN6, the nitrogen blend at 4604–4640 Å, for WR 110 and WR 36, appears to be dominated by N v 4604, 4620 rather than N iii 4634, 4630. Note also that, for WR 36, the emission above 4900 Å appears to be He I rather than N iv 4940.

designation includes two possibilities: that the star is a spectroscopic binary; or there is an unrelated star near enough on the sky to be unresolved at the spectrograph, i.e., a close optical pair. If the pair is visually resolved, we enclose the OB star classification in brackets.

The ‘a’ designation is applied only to the type of spectra in which violet-shifted absorption edges belonging to the WR spectrum can be confused with absorption lines from a companion. Specifically, the Balmer and Pickering emissions are weak, and the EWs of the absorption edges are comparable to the EWs of the emission. The line profiles are intermediate between those of an O absorption spectrum and a well-developed WR emission spectrum; the absorption lines are nearly filled in, but the emission is not dominant. No such case is known without hydrogen being present; thus the ‘a’ designation necessarily goes with ‘h’. If apparently undisplaced absorption is present, usually in the higher Balmer lines, but the emission spectrum indicates no hydrogen, we assume that absorption lines come from a companion, gravitationally bound or otherwise, and the spectral classification is ‘+ OB’.

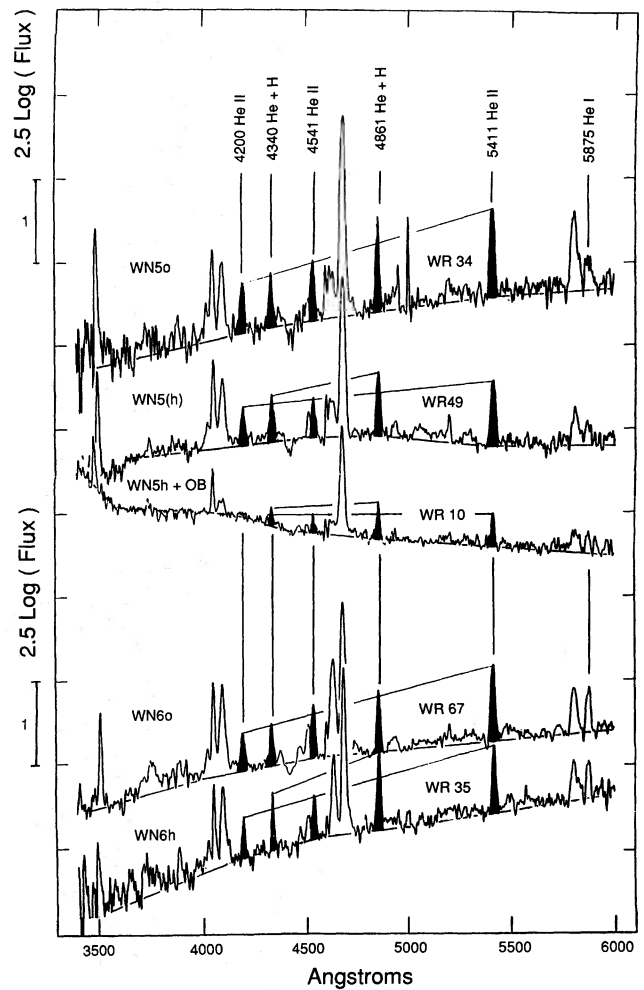


Figure 6. Examples of WN5 and WN6 stars with no hydrogen, ‘o’, marginal hydrogen, ‘(h)’, and definite hydrogen, ‘h’. The five strong Pickering lines used for H^+/He^{++} estimation are shaded, and the peaks of lines with and without hydrogen contribution are joined to enhance the visibility of the criterion used.

The ‘a’ designation is not applied to spectra in which the emission is strong relative to the violet absorption component and in which the absorption has a large displacement. High-dispersion spectra of Crowther et al. (1995a, figs 2 and 3) clearly demonstrate the difference between the spectra now designated ‘ha’, WR 108 (WN9ha) and WR 24 (WN6ha), and a fully developed WR spectrum with violet absorption edges, WR 16 (WN8h). Crowther (private communication) suggests that the clearest single discriminant is the 4340 ($H\gamma + He II$) line which has nearly equal emission and absorption EWs in ‘ha’ spectra and is mostly emission in other WR spectra.

WR 22, 24 and 25 are the archetypical ‘ha’ stars. With good signal-to-noise ratio, they can, in principle, be assigned an ionization subclass from the $He II/He I$ ratio. However, the lines are very narrow, and the result, using peak line/continuum, is acutely resolution-dependent! Low resolution, like that of the TM88 spectra, will place WR 22 in WN7 and WR 24 and 25 in WN6 (as suggested by Walborn 1974). At high resolution, WR 22 would also be classified WN6. We classify them by the ratios obtained at the lower

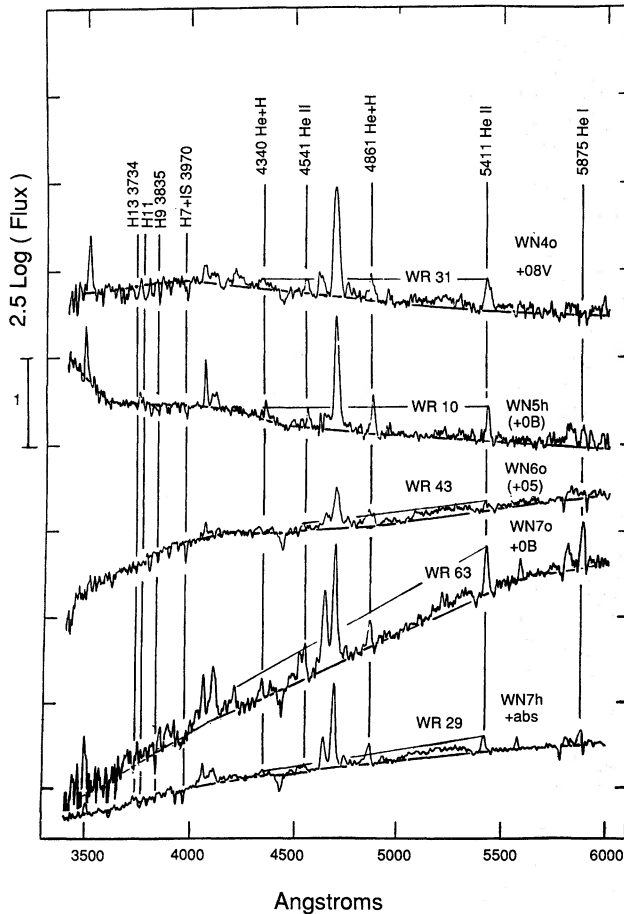


Figure 7. Some spectra with absorption lines.

resolution, but consider the situation to be less than totally satisfactory.

3.5 WN/C spectra

Some WN stars show stronger than normal C iv 5808 or C iii 5696 (for a recent list see Conti & Massey 1989, hereafter CM89) superposed on an otherwise fairly normal WN spectrum. Initially suspected of being binary WR stars, it has since been shown (e.g., Massey & Grove 1989; Crowther et al. 1995e), for most of these objects, that the N and C lines probably come from the same star. If the spectra were a superposition of two normal spectra from a WN and a WC star, the WC subclass could be determined from the ratio C iv 5808/C iii 5696. Most WN/C stars show strong C iv 5808 with little or no C iii 5696. The large ratio C iv 5808/C iii 5696 implies WC4 or WC5. However, the ratio C iv 5808/4650 is generally also large, a situation which does not occur in any fully developed WC spectrum. WO stars can have C iv 5808/4650 $\gg 1$ (Smith, Shara & Moffat 1990a), but line widths in WO stars are also large, of the order of 100 Å, which is not observed in the WN/C stars. Only the lowest excitation WN/C star, WR 98, has ratios of 5808/5696/4650 which approximate those for a WC7 star, although the widths of the C lines are lower than average for that subclass. Accordingly, only for WR 98 is the /C spectrum given a subclass number; the high-excitation stars are

left with the classification '/CE' as given by CM89. The abnormality of the 'WC' spectrum appears to eliminate any remaining possibility that these stars can be explained by the presence of two WR stars, one WN and one WC.

4 THE IONIZATION SUBCLASSES

WN2. Demarcated by absence of N iv and N v (N iii is also absent as for WN3). There is only one Galactic (WR 2) and one LMC (Br 4) star known in this class. The visible spectrum is dominated by very broad He ii lines.

WN2.5. This subclass, 'reluctantly' suggested by CM89 because of undetectable N iv 4057 in the spectra of Br 6 and 16, disappears from the new system. What is extraordinary about Br 6 and 16 is the line width, not the ionization. N iv 4057 is probably present (at least in Br 16) but hard to see in the blend between 4026 and 4100 because the lines are so broad. He i 5875 is present and gives He ii/He i less than 10; and C iv 5808 is clearly present, excluding an ionization subclass earlier than 4. We classify both stars WN4b, and it is likely that Br 16 has a superposed OB spectrum.

WN3. Demarcated by weak or absent He i 5875 and C iv 5808, but N v present and strong. This subclass is poorly represented in the Galaxy. There are only four: WR 3, 46, 127 and 152. WR 3 has a clear O spectrum superposed (Smith & Kuhi 1981), but is otherwise identical to WR 46 (Fig. 2). WR 46 (SB1) has very weak emission lines compared to stars of comparable line width in the LMC, suggesting that its companion is not seen in the combined spectrum, which is classified 'pec'. WR 3 and 46 are remarkable in the strength of the N v 4604,20 doublet relative to He ii 4686. The He/N EW ratio (see Fig. 11) of WR 152 and the binary star WR 127 are comparable to those of the LMC stars. The narrow-lined star WR 152 appears to have some hydrogen, and falls on the lower end of the EW-WHM relationship defined by the LMC stars (see Fig. 17).

The profiles of the lines in the spectra of the Galactic WN3 stars are triangular rather than Gaussian. The widths given in Table 6 and plotted in the diagrams are the FWHM with maxima taken at the top of the triangle; the values are significantly narrower than obtained using a Gaussian fit which cuts off the top of the profile. Severe differences in FWHM given by different observers is probably due to inconsistency in defining HM. The LMC WN3 stars have Gaussian profiles.

WN4. Demarcated by He ii/He i between 4 and 10 (0.6 and 1.0 dex) and N iv 4604 $> 2 \times$ N iii 4640 (peak fluxes). Presence of C iv 5808 is a very useful discriminator against WN3. The most extreme star, WR 128, on the border to WN3, also has triangular line profiles. Otherwise, the Galactic and LMC WN4 stars are similar. Fig. 4 shows the 4600 region for two WN4b spectrum compared to a WN40 spectrum; the main difference is the width and strength.

WN5. Demarcated by N v 4604 = N iii 4640 (peak fluxes), within a factor of 2, and N iv 4057 and/or C iv 5808 $>$ He i 5875 is a useful subsidiary indicator. This class comprises spectra previously called WN4.5. They are unusually uniform in all properties investigated; the tight correlation of the He/N ratio with $R(\text{Gal})$ is particularly striking (Fig. 11). The number of '+OB' composite spectra is high. In the Galaxy, the fraction is 8/19 \sim 42 per cent,

Table 5. Observed and expected numbers of binaries by ionization subclass.

Subclass	Galaxy			LMC-new subclasses only		
	Total	Binary 1)	Expected	Total	Binary 1)	Expected
WN2	1	0	0.2	1	1	0.2
WN3	4	2	0.9	8	0	1.8
WN4	12	2	2.6	24	3	5.3
WN5	19	8	4.2	7	6	1.5
WN6	16	4	3.5	5	0	1.1
WN7	17	2	3.7	3	1	0.7
WN8	14	0	3.1	3	0	0.7
Total	83	18		51	11	
Fraction	0.22			0.22		
Probability of Chi-squared	0.16			0.002		

(1) + abs are not counted as binary.

compared to the overall average, 22 per cent. A chi-squared test on the distribution of binaries by ionization subclass (Table 5) gives a probability of 0.2, which is not significant. However, in the LMC, six out of seven of the spectra classified WN5 are composite. A chi-squared test gives a probability of 0.03, entirely due to higher than expected numbers of WN5 binaries. Data in the LMC are incomplete, but all other stars classified WN4.5 or WN5 by Breysacher (1981) are also listed as + OB. No explanation is apparent.

WN5b. Only two single stars, WR 36 and 110, have been tentatively assigned to this class. The $N\text{v } 4606/N_{\text{III}} 4640$ criterion is almost impossible to apply. Fig. 5 shows the 4600 region of the WN5b and WN6b spectra in our collection. For WR 36 and 110, $N\text{v}$ appears to dominate. However, $\text{He II}/\text{He I}$ is at the bottom of the range for WN5, and neither $N\text{IV } 4057$ nor $\text{C IV } 5808$ is as strong as for most narrow-line WN5 stars; in the classification diagrams, Figs 9 and 10, they fall among the WN6 stars. For these reasons, we assign an intermediate classification of WN5–6b.

WN6. Demarcated by $\text{He II}/\text{He I}$ between 1.25 and 4 (0.1 and 0.6 dex) and $N\text{v } 4606 < 0.5 \times N_{\text{III}} 4640$ (peak fluxes). $\text{C IV } 5808 \sim \text{He I } 5875$ is a useful subsidiary indicator. Fig. 5 shows the 4600 region for a WN6b spectrum compared to a WN6o spectrum; the main difference is the width and strength.

WN7. Demarcated by $\text{He II}/\text{He I}$ between 0.65 and 1.25 (–0.2 and 0.1 dex). $\text{C IV } 5808 < \text{He I } 5875$ is a useful subsidiary indicator.

WN8. Demarcated by $\text{He II}/\text{He I}$ between 0.1 and 0.65 (–0.1 and –0.2 dex), but the lower boundary is uncertain. $\text{He I } 4471$ becomes comparable to or stronger than $\text{He II } 4541$. The latter ratio has not been quantified, because $\text{He I } 4471$ cannot be reliably measured in earlier subclasses. However, if only a blue spectrogram is available, it is a useful indicator. $\text{C IV } 5808$ is weak or absent. Strong violet absorption on the He I lines is common in WN8, but is not exclusive to this subclass.

WN9–11. See Crowther et al. (1995a).

5 CLASSIFICATION OF GALACTIC AND LMC WN STARS ON THE NEW SYSTEM

Table 6 lists all WN stars in the van der Hucht et al. (1988, hereafter VdH88) catalogue. Companion star classifications

are taken from the Smith & Kuhl Atlas (1981) or from the authors who made the binary analysis, as referenced in column [7]. Visual companions (from VdH88) are included in the spectral classification (in brackets), since their light contributes to most spectrograms.

Columns [1] and [2] give the numbers in the van der Hucht et al. (1981), HD and other catalogues. [3] and [4] give classifications from VdH88 and HS66. [5] gives classifications for the WR or companion star which differ from those in columns [3] and [4], with references in column [7]. [6] gives the binary status with a reference in column [7]. The reference chosen is usually to a recent paper with current information. [7] gives references for data in columns [5] and [6]. [8] gives the classification of the new system. [9] flags an individual (*) or generic (numbers) comment at the end of the table. [10] gives the source of the spectra we have examined. The TM88 and Hamann, Koesterke & Wessolowski (1995) spectra were provided in hard copy by Paul Crowther, together with the spectra from his thesis (Crowther 1993) and more recent acquisitions (Crowther, private communication). [11] gives *FWHM* 4686 taken from the highest resolution source listed in column [10]. When only a TM88 spectrum was available, the *FWHM* given by CM89 is flagged ‘corr’ and is corrected for a spectroscopic resolution of 12 Å (TM88 states ‘10–15’); this correction gives good agreement with higher resolution observations when they are available. ‘var’ indicates scatter in EW or *FWHM* measurements which appears to be above the observational uncertainty; these are discussed in Section 9. [12] gives EW 5411 from the same source as [11]. [13] gives $\text{H}^+/\text{He}^{++}$ from the HKW, CLP, this paper – Table 3, or estimated from the spectra listed in column [10]. Columns [14]–[17] give line ratios (using the peak line/continuum measure. For stars not observed, the values have been measured from a hard copy of the TM88, Hamann et al. (1995) or Crowther spectra; these are less accurate than could be done in digital form on a computer, but are the ‘ruler’ estimates from which the classification was assigned. [18] gives $\log \text{EW}(\text{He II } 4686/N_{\text{V,III}} 4604\text{--}40)$ from CM89, CLP or our spectra. We use EW in this case to make use of extensive data available in the literature.

Table 7 lists all WN stars in the Breysacher (1981) catalogue of the LMC. Our limited sample of LMC WN spectra is shown in Fig. 8. The majority of the new classifications are made from TM88 spectra in public access, provided to us in hard copy by Crowther and from new spectra (Crowther, private communication). The information is similar to that in Table 6. Classification of companions is from previous authors except where otherwise noted.

6 LINE RATIOS AND IONIZATION SUBCLASS

6.1 Classification ratios

The primary ionization subclass criterion is the ratio of $\text{He II } 5411/\text{He I } 5875$. $N\text{v } 4604/N_{\text{III}} 4640$ is also a primary criterion for discrimination of WN4/5/6, but is poorly defined outside those classes. Strengths of $N\text{IV } 4057$ and $\text{C IV } 5808$ relative to appropriate lines, while not primary criteria, have

Table 6. Classification of all Galactic WN stars in the van der Hucht et al. (1988) catalogue.

WR#	HD or VdH81	Spectrum										Peak/Continuum ratios					log EW
		HS66	VdH88	Other	Binary status	Ref. [5,6]	New Class	Note	Source	FWHM 4686 (A)	EW 5411 (A)	H \pm He++	HeII 5411 HeI 5875	HeII 4057 N 4604-40	HeII 5808 HeI 5875	4686	
[1]	[2]	[3]	[4]	[5]	[6]	[7]	[8]	[9]	[10]	[11]	[12]	[13]	[14]	[15]	[16]	[17]	[18]
1	4004		WN5				WN4b		2	38	67	0	3.7	0.6	0.7	2.8	0.87
2	6327		WN2				WN2b		2	63	40	0	>10	0.1	0.0	0.0	..
3	9974		WN3+ α	WN3+O4	SB1?	A,ML86	WN3b+O4	*	A,2	31	8	0	>10	0.1	0.0	0.0	0.13
6	50896	WN5-B	WN5		SB1?	RM92	WN4b		A,2,1,3	36	var	68	0	5.3	0.6	0.4	0.66
7	56925	WN5-B	WN4				WN4b		2,1,3	30	75	0	10	0.2	0.4	4.4	0.68
8	62910	WN7-B	WC4/N6		SB1?	WS90	WN7o/CE		1,2	22	var	25	0	1.1	0.2	3.9	..
10	65865	WN5.5-A	WN4.5	WN4.5(+OB)	visual	VdH88	WN5h(+OB)		1,3	20	8.2	0.5	2.5	4.3	0.5	1.3	0.91
12	MR13		WN7		SB1	NI82	WN8h		1,3	18	12	1.3	0.4	0.5	0.2	0.1	0.29
16	86161		WN8				WN8h		2,1,3	8	5.1	2.6	0.3	0.2	0.2	0.1	0.04
18	89358		WN5				WN4b		2,3	44	var?	73	0	6.7	0.6	0.7	0.79
20	BS1		WN4.5				WN5o		1,3	24	39	0	2.3	2.6	1.0	2.2	0.79
21	90657		WN4+O4-6		SB2	NM82	WN5o+O4-6	*	3	27	6	0	2.4	1.4	1.1	1.6	0.75
22	92740		WN7+ α		SB1	MS78	WN7ha	1	2,3	13	3.5	4	1.6	0.4	0.4	0.7	0.29
24	93131		WN7+ α				WN6ha	1	2,3	17	4.2	1	3.2	2.0	0.8	2.5	0.53
25	93162		WN7+ α				WN6ha	1	2,3	18	1.9	2	3.3	2.3	1.0	3.3	0.37
26	MS1		WN5/C	WCE/N5		CM89	WN7b/CE	*	1,3	52	81	0	1?	0.2	8.3	10	0.21
28	MS2		WN7				WN6(h)		1,3	18	11	0.4	3.3	0.9	0.5	1.7	0.51
29	MS3		WN7				WN7h+abs		1,3	18	4.1	0.6	1.0	0.7	0.5	0.5	0.48
31	94546		WN4+OBV		SB2	NM85	WN4o+OBV		1	28	12	0	8?	0.7	0.94
34	LS5		WN4.5				WN5o		1	24	38	0	3.8	2.5	0.8	3.2	0.82
35	MS6		WN6				WN6h		1,3	17	20	0.5	2.4	1.1	0.5	1.2	0.49
36	LS6		WN4				WN5-6b	*	1,3	47	var	65	0	1.2	1.0	0.7	0.88
37	MS7		WN3				WN4b	*	3,6	44	56	0	3.8	0.4	0.6	2.5	0.83
40	96548		WN8				WN8h		2,3	12	8.7	2	0.4	0.2	0.1	0.0	0.09
43	97950		WN6+O5		cluster	NM84	WN6o(+O5)	*	1,3	26	var?	3	0	1.6	1.1	1.4	0.50
44	MR39		WN4				WN4o		1	28	37	0	6.8	0.6	0.5	3.4	0.77
46	104994		WN3p		SB1	NB95	WN3b pec	3,*	2,1	36	var	15	0	>10	0.1	0.0	0.19
47	311884		WN6+O5V		SB2	NC80	WN6o+O5V		3	23	corr	14	0	1.4	0.8	0.5	0.73
49	LSS2979		WN5				WN5(h)		1,3	22	25	0.4	3.5	2.9	0.5	1.8	0.72
51	MR45		WN4				WN4o		1,3	25	26	0	6.7	1.0	0.4	2.6	0.73
54	MR48		WN4				WN5o		3b,6	25	30	0	6.8	1.9	0.4	2.6	0.61
55	117688		WN7				WN7o		1	17	26	0	1.0	0.6	0.4	0.5	0.22
58	MR51		WN4	WN4/CE		CM89	WN4b/CE		3	34	corr	68	0	8?	0.9	1.6	0.60
61	MR53		WN4.5				WN5o		1,3	27	36	0	4.9	1.7	0.7	3.6	0.57
62	NS2		WN6				WN6b		1	34	55	0	1.7	0.5	0.4	0.7	0.41
63	LSS3289		WN6	WN7		CM89	WN7o+OB	*	1,3	18	12	0	1.0	0.6	0.5	0.5	0.14
66	134877		WN8		SB1?	AB95	WN8(h)	*	3,6	18	11	0.2?	0.4	0.2	0.1	0.1	0.05
67	MR55		WN6				WN6o		1,3	22	30	0	2.2	0.9	0.5	1.0	0.23
71	143414		WN6		SB?	IM83	WN6o		1,3	24	36	0	3.6	0.8	0.4	1.4	0.27
74	BP1		WN7				WN7o		1	17	21	0	0.9	0.7	0.4	0.4	0.08
75	147419		WN6				WN6b		2	45	57	0	1.5	0.6	0.3	0.5	0.42
78	151932	WN7-A	WN7				WN7h	*	A,2	13	8.3	1	1.2	0.6	0.3	0.4	0.26
82	LS11		WN8				WN7(h)		3,6	15	14	0.4	0.8	0.6	0.2	0.2	0.05
83	MR67		WN6				WN5o	*	3	21	corr	21	0	4.5	1.9	0.4	0.38
84	LS12		WN6				WN7o		1,3,6	17	21	0	1.2	0.7	0.4	0.5	0.17
85	155603B		WN6				WN6h		3	16	corr	15	0.6	2.7	0.9	0.3	0.21
87	LSS4064		WN7	WN8+OB		HM77	WN7h+abs	2	3,6	12	4	1?	0.9	0.1	0.5	0.3	0.03
89	LSS4065		WN7	WN8+OB		HM77	WN8h+abs	2	3,6	11	0.9	2?	0.5	0.1	0.2	0.1	0.07
91	StSa1		WN7				WN7b	3	1,3	32	32	0	0.8	0.7	0.5	0.4	0.24
94	158860		WN6				WN5o		3b	22	corr	0	..	1.0	0.43
97	320102		WN3+O5-7	WN4+O7	SB2	NI95	WN5b+O7	*	3	32	corr	4	0	abs'n	0.8	0.7	..
98	318016		WN7/C7		SB1	NI91	WN8o/C7		3	21	corr	13	0	0.5	..	1.9	1.0
100	318139		WN6				WN7b		3b,6	32	46	0	1.2	0.6	0.4	0.4	0.21
105	NS4		WN8				WN9h		2	8	0.6	7	0.1	-0.15
107	DA1		WN7-8				WN8o	*	3b	9	corr	0?	..	0.6	-0.09
108	LS14		WN9				WN9ha		2,1,3	5	0.3	2?	0.3	0.1	0.0	0.0	-0.26
109	NS3		WN3				WN5h	*	4	24	26	1	2.8	0?	0.4	1.0	..
110	165688	WN6-B	WN6				WN5-6b	*	2,1,3	59	var?	68	0	1.9	0.6	0.5	0.8
115	MR87		WN6				WN6o		1,2	19	20	0	2.3	0.8	0.5	0.8	0.34
116	St1		WN8				WN8h	*	5,6	12	3.5	>4	0.1	..	0.4	<0.1	-0.09
120	MR89	WN7-A	WN7				WN7o		2,6	14	15	0	0.7	0.4	0.3	0.2	0.05
123	177230	WN8-A	WN8		SB1?	LM83	WN8o		2	13	8.9	0	0.3	..	0.3	0.1	-0.22
124	209BAC		WN8		SB1?	ML82	WN8h		2	12	4.1	2	0.1	..	0.0	0.0	-0.10
127	186943	WN5-A	WN4+O9.5V	WN4+O9/B0V?	SB2	Ma81	WN3b+O9.5V	4	..	30	corr	12	0	large	0.82
128	187282	WN5-A	WN4		SB1?	VdH88	WN4(h)	*	A,2	25	17	0.4	9.1	0.3	0.2	2.0	0.64
129	MR96		WN4				WN4o		6	25	31	0	8.7	1.0	0.6	5.0	0.95
130	LS16		WN8				WN8(h)		6	10	5	0.4	0.4	0.1	0.2	<0.1	0.08
131	MR97		WN7+ α				WN7h+abs	2	2,6	13	3.1	0.8	1.2	..	0.2	0.3	0.33
133	190918	WN5.5-A	WN4.5+O9.5Ib:	WN4.5+O9I	SB2	A,UH94	WN5o+O9I		A,2	28	3.7	0	3.3	..	1.6	0.9	2.9
134	191765	WN6-B	WN6		SB1?	MB94	WN6b		2	43	65	0	3.4	0.8	0.5	1.5	0.61
136	192163	WN6-B	WN6		SB1?	KF80	WN6b(h)	*	A,2	33	58	0.4	2.9	0.7	0.3	0.7	0.54
138	193077	WN6-A	WN6+ α	WN6+O9	SB2	An91	WN5o+B?	*	A,2	22	13	0	4.0	1.5	0.3	1.2	0.69
139	193576	WN6-A	WN5+O6		SB2	MM94	WN5o+O6	*	2	24	9.7	0	4.2	..	0.8	3.1	0.73
141	193928	WN6-B	WN6	WN6+OB	SB2	GM91	WN5o+OB		2	27	32	0	2.6	..	0.6	1.5	0.65
145	MR111		WN7/C4		SB1	MG89	WN7o/CE+OB?	3,*	2	22	10.5	0	1.0	0.3	4.3	4.3	-0.01
147	NS6		WN7	WN8		CM89	WN8(h)	*	6	11	5	0.2?	0.3	..	0.2	<0.1	0.14
148	197406	WN7-A	WN7		SB1	Mo92	WN8h		2,6	10	2.6	1?	0.6	0.3	<0.1	<0.1	0.35
149	St4		WN6				WN5o		6	20	39	0	3.0	1.3	0.6	1.7	0.61

Table 6 — continued

WR#	HD or other	H566	VdH88	Other	Spectrum					FWHM 4686	EW 5411	Peak/Continuum ratios						log EW 4686
					Binary status	Ref [5,6]	New Class	Note	Source			H+	HeI 5411	NIV 4057	QIV 5808	QIV 5808		
VdH81										(A)	Note (A)	He++	HeI 5875	N 4604-40	HeI 5411	HeI 5875	4640	
[1]	[2]	[3]	[4]	[5]	[6]	[7]	[8]	[9]	[10]	[11]	[12]	[13]	[14]	[15]	[16]	[17]	[18]	
151	CX Cep		WN4+O8V	WN4+O5V	SB2	LM93	WN4o+O5V	4	..	25	corr	19	0	6 :	1.09	
152	211564	WN4-A	WN3				WN3(h)	*	2	26		20	0.4?	10	0.1	0.1	>1	
153	211853	WN6.5-A	WN6+O+..	WN6/CE+O	quad	CM89, Ma81	WN6o/CE+O6I	*	A,2	20		9	0	2.6	0.7	2.6	0.59	
155	214419	WN7-A	WN7	WN6(h)+O9II/lb	SB2	Ma94, Ni80	WN6o+O9II/lb	*	2	18		3.4	0	1.4	..	0.4	0.46	
156	MR119	WN8-A	WN8				WN8h	*	A,2	6		2.1	4	0.2	0.2	0.8	0.05	
157	219460	WN5.5-A	WN4.5	WN4.5+B1II	visual	VdH88	WN5o(+B1II)	*	2,6	20		15	0	6.5	3.1	0.3	2.3	
158	MR122		WN7				WN7h		6	10		3.8	1.4	1.0	0.5	0.3	0.18	

Notes to Table 6

Column [6]: Binary status

SB2 Radial velocity variations seen for both components.

SB1 Radial velocity variations seen for WR star only.

visual The stars are resolved, probably not related.

.. Nothing in column 6 with + OB (or more specific) in the classification, column 8, means a spectrum binary but no known radial velocity variations.

i.e. absorption lines are visible (usually the high number Balmer lines) and the Pickering decrement is smooth for the emission lines.

Column [7]: References for binary status and differing classification.

A	Smith-Kuhi Atlas (1981)	LM83	Lamontagne et al. (1983)	MM94	Marchenko et al. (1994)	Ni95	Niemela (1995)
An91	Annuk (1991)	LM93	Lewis et al. (1993)	Mo92	Moffat (1992)	NM82	Niemela & Moffat (1982)
AB95	Antokhin et al. (1995)	Ma81	Massey (1981)	MS78	Moffat & Seggewiss (1978)	NM85	Niemela et al. (1985)
CM89	Conti & Massey (1989)	Ma94	Marchenko (private communication)	NB95	Niemela et al. (1995a)	RM92	Robert et al. (1992)
GM91	Grandchamp & Moffat (1991)	MB94	McCandliss et al. (1994)	NC80	Niemela et al. (1980)	UH94	(Underhill & Hill (1994)
HM77	Havlen & Moffat (1977)	MG89	Massey & Grove (1989)	Ni80	Niemela (1980)	VdH81	Van der Hucht et al. (1981)
HS66	Hiltner & Schild (1966)	ML82	Moffat et al. (1982)	Ni82	Niemela (1982)	VdH88	van der Hucht et al. (1988)
IM83	Isserstedt et al. (1983)	ML86	Moffat et al. (1986)	Ni91	Niemela (1991)	WS90	Willis & Stickland (1990)
KF80	Koenigsberger et al. (1980)	MN84	Moffat & Niemela (1984)				

Column [9]: Notes to Galactic spectra.

- WR22, 24 and 25. TM88 spectra indicate He II 5411/He I 5875 < 1 for WR22 and definitely > 1 for WR 24 and 25. High-resolution spectra (Crowther et al. 1995b) give peak/continuum ratios of 0.6, 0.14 and 0.4 respectively. See text: the quantitative classification fails for these stars.
- N IV 4057 and He II 5411 very weak and narrow. Data quoted is a mixture from sources quoted. *EW* 5411 and *FWHM* 4686 all into the range of 'ha' stars.
- Lines weak for their width (see Fig. 16 and Table 8) suggesting the presence of a companion.
- No spectrum sighted. Ionization subclass from *EW* ratio of He II 5411/He I 5875 multiplied by 1.25 (see Section 3.1); H⁺/He⁺⁺ from CLP.

*Notes to individual spectra:

- The Smith-Kuhi Atlas (1981) shows absorption lines centrally placed on the emission.
- CLP gives H⁺/He⁺⁺ = 0.4; TM88 spectrum shows no hydrogen. Lines are seriously affected by the O spectrum; Pickering decrement is unreliable.
- He II 4686 is blended with C III 4650; the *FWHM* given is for He II 5411. He I 5875 is affected by C IV 5808.
- See fig. 5 for detail of 4600 Å region. See Section 4 for discussion of the classification.
- EW* 5411 measures are divergent. CM89 give 78Å which is as expected for the *FWHM* 4686 (see Fig. 16).
- CM89 give *FWHM* 4686 = 35 Å, which would give a 'b' classification. Strong C IV 5808 on our spectrum indicates some WN5 component to this composite spectrum.
- O VI 3811,34 strong relative to He II 4686.
Our spectrum indicates marginal hydrogen presence; however, TM88 spectrum and HKW indicate no hydrogen.
- Our spectrum shows Balmer absorption at H9,3835 and possibly at H11 and 13.
- 4541 is unusually strong, making H⁺/He⁺⁺ uncertain.
- He II/I = 1.25 is on border to WN6; however, all secondary indicators give WN7.
- Weak narrow lines (see Fig. 16) suggest that hydrogen is probably present below the detection limit for the (rather noisy) TM spectrum.
- He I 5875 is affected by absorption. N IV 4057 is not strong, but C IV 5808 is strong, as required for WN5.
- TM88 have blue spectra only, WN8 rather than WN7 on the basis of He II 4541/He I 4471.

Notes to Table 6 — *continued*

- 109 From spectrum given by Lundstrom & Stenholm (184a). N iv 4057 appears to be missing, hence their classification of WN3.
 110 As for 36.
 116 Borderline WN9. N iv 4057 and He II 5411 very weak. O III 5696 strong.
 128 The most extreme WN4 star. He I too weak to measure; however presence of N iv and C iv indicate WN4 rather than WN3. Lines are triangular, like Galactic WN3 spectra.
 136 10 per cent by mass hydrogen content confirmed by Crowther & Smith (1995).
 138 HKW report possible hydrogen detection.
 139 V444 Cyg.
 145 H β is weak relative to He II 4541 and He II 5411 and has structure suggesting the presence of superposed absorption.
 147 4861 appears to be affected by noise or nebular emission, 4340 not recorded, making H $^+$ /He $^{++}$ uncertain.
 152 Crowther's spectrum shows no sign of H, but both CLP and Hamann et al. (1955) record a detection.
 153 GP Cep. Smith (1973) gives H $^+$ /He $^{++}$ = 0.35 \pm 0.25; the detection is unconvincing. The O spectrum makes the Pickering decrement unreliable. O61 is from A.
 155 CQ Cep. Ma94 finds H $^+$ /He $^{++}$ = 0.2 \pm 0.1.
 156 C III 4650 resolved from N III 4640; Crowther et al. (1995b) find slightly enhanced C/N ratio. Narrowest line WN8 star known.
 157 No sign of the B companion on Crowther's spectrum and his *EW*s are twice those given by CM89.

Column [10]: source of spectrum used for classification.

- A Smith-Kuhi Atlas (1981); resolution 1–3 Å.
 1 From new spectrum, this paper; resolution 4–6 Å.
 2 Our inspection of spectra from Crowther 91993) or more recently obtained (Crowther, private communication); resolution 2–3 Å.
 3 Our inspection of TM88 spectrum; 3b=blue only. *FWHM* 4686 and *EW* 5411 from CM89; resolution 10–15 Å.
 4 Lundstrom & Stenholm (1984a).
 5 Lundstrom & Stenholm (1984b).
 6 Hamann et al. (1995) data; *FWHMs* and *EW* measured by Crowther (private communication); resolution 1–2 Å.

Column [11]: notes to *FWHM* 4686.

var *FWHM* 4686 or *EW* 5411 have reported values differing by significantly more than usual errors; see Section 9.

corr *FWHM* 4686 is taken from CM89 and corrected for an instrumental resolution of 12 Å; see Section 5.

Table 7. Classification of LMC WN stars in the Breysacher (1981) catalogue.

Br#	Spectrum									FWHM		EW		Peak/Continuum ratio				log EW
	Br81 (Me78, Wa77)	CM89 CLP	Other	Binary Status	Ref [4,5]	New Class	Note	Source		4686 (A)	Note	5411 (A)	He++	He I 5411 He I 5875	C IV 5808 He I 5411	C IV 5808 He I 5875	4686	
[1]	[2]	[3]	[4]	[5]	[6]	[7]	[8]	[9]		[10]		[11]	[12]	[13]	[14]	[15]	[16]	
1	WN3	WN3				WN3b		3,4	36	5411		58	0	>10	0.0	0.0	0.72	
2	WN4	
3	WN3	WN4				WN4b	*	2,3	27			43	0	9.5	0.3	2.3	0.70	
4	WN4	WN2				WN2b+OB?	*	3,4	35	5411		41	0	>10	0.0	0.0	..	
5	(WN5-6A+O6-7n-nn)		O3f*+O8-B0I	SB2	NS95	
6	WN3p	WN2.5				WN4b	*	2,3,4	63			85	0	12.5	0.3	3.0	..	
11	WN4+OB?	
12	WN3	WN4		const RV?	Mo95	WN4b		2,3,4	33			63	0	5.9	0.5	2.7	0.75	
13	WN8	WN8		const RV	Mo89	WN8h		1,2,3,4	13			10	1.7	0.6	0.2	0.1	0.37	
14	WN4	WN4				WN4o		1,3	25			33	0	5	0.6	4.4	0.66	
15	WN4	WN4				WN4(h)		3	26	corr		23	0.5	..	0.4	..	0.77	
16	WN3-4p+OB?	WN2.5				WN4b+OB?	*	2,3,4	52			43	0	5.9	0.4	2.0	0.95	
17	WN4+OB	WN3+abs		const RV?	Mo95	
18	WN9-10	WN9		const RV	Mo89	WN9h		2,3	6			0.5	>30	0.05	-0.22	
19	WN3	WN4				WN4b		3	52	corr		89	0	7.1	0.4	2.6	0.72	
20	WN4	WN4				WN4b		3	29	corr		55	0	5.0	0.8	4.0	0.66	
21	B2I+WN3	B1Ia+WN3		SB2?	Mo95	WN5?b+B1Ia	*	3	37	corr		0	0	..	1.1	..	0.89	
23	WN3	WN3		var RV?	Mo95	WN4b		3	29	corr		50	0	4.8	0.5	2.3	0.71	
24	WN7	WN7				WN6h		1,2,3,4	13			10	1.3	2.3	0.4	0.9	0.54	
25	WN3	WN3				WN3b	*	..	31	corr		60	0.69	
26	WN7	WN7		SB1	Mo89	WN6(h)+abs?	*	1,2,3,4	20			17	0.3	2.4	0.3	0.7	0.86	
27	WN3	WN3				WN3o	*	3,4	27	5411		34	0	20	0.1	>2.5	0.61	
29	WN4p	WN3/CE		const RV?	Mo95	WN4b/CE		2,3,4	33			49	0	5	7.8	..	0.87	
30	WN3:	..				WN4b	*n	3	31	corr		..	0	8.3	0.4	3.7	..	
33	WN3+OB	WN3+a				WN5o+O	*n	3	25	corr		12	0	1.4	1.3	2.0	1.00	
34	B3I+WN3:	B3I+WN3		SB?+visual	Mo95	WN5?b+(B3I)	*	3	59	corr		..	0	..	0.0	0.0	..	
35	WN4	WN4				WN4b		3	26	corr		63	0	7.1	0.6	4.0	0.83	
36	WN8	WN8				WN8h		2,3	8			4	1.9	0.6	0.3	0.2	0.18	
37	WN3+OB	WN3+a		SB2	Mo95	WN4+OB		4	27	5411		21	..	7.1	0.4	2.6	0.93	
38	WN3	WN4				WN4o		3	29	corr		32	0	6.3	0.3	2.0	0.74	
39	WN3	
40	WN3	WN4				WN4b		3,4	31	5411		53	0	5.9	0.5	3.2	0.69	

Table 7 — *continued*

Br#	Spectrum								FWHM		EW	Peak/Continuum ratio					log EW
	Br81 (Me78)	CM89 CLP	Other	Binary Status	Ref [4,5]	New Class	Note	Source	4686 (A)	Note	5411 (A)	H+ He++	HeII 5411 HeI 5875	CIV 5808 HeII 5411	CIV 5808 HeI 5875	4686 4640	
[1]	[2]	[3]	[4]	[5]	[6]	[7]	[8]	[9]	[10]		[11]	[12]	[13]	[14]	[15]	[16]	
41	WN4.5+OB
42	WN3	WN3				WN3b		3	46	corr	81	0	10.0	0.0	..	0.89	
44a						WN8h	*	2	6		0.5	57	0.3	<0.2	< 0.1	..	
45	WN3	WN3				WN4b		3	32	corr	66	0	6.3	0.6	4.0	0.64	
46	WN3	WN4				WN4b		3	30	corr	46	0	>10	0.7	..	0.61	
47	WN8	WN8				WN6h		2,3,4	12		9	0.9	1.8	0.5	0.9	0.48	
48	WN4+OB	WN3+a		const RV?	Mo95	WN4o?+B	*,n?	3,4	29	5411	9	0	5.0	0.5	2.3	0.65	
49	WN3+OB	WN3+a				26	corr	0.0	..	0.87	
51	WN3	WN3				WN3o	*	3	27	corr	32	0	10	0.0	0.0	0.49	
52	WN4+OB	WN4+a		const RV?	Mo95	WN4h+abs		2,3,4	26		11	0.7	12	0.4	5	0.88	
53	WN4+OB?	
54	WN3	WN3				WN3b(h)		3	30	corr	23	0.5	>10	0.0	0.0	0.53	
55	WN4	
56	WN5:	WN6				WN5o?+OB	*,n	2,3,4	23		6	0?	7	0.5	3.0	1.00	
57	WN6	WN7				WN7h+OB	*	2,3	15		7	0.9	0.9	0.1	0.1	0.37	
58	WN5-6	WN5-6				Of		3	21	corr	
59	WN3	
60	WN3	WN3				WN3o pec	*	3	23	corr	7	0	>10	0.0	0.0	0.76	
61	WN3-5	
63	WN4.5+OB	
64	WN9 -10	WN9				WN9h		2,3,4	5		0.5	..	0.1	0.0	0.0	-0.02	
65	WN/Of?	..	WN7	SB1+cluster	Mo89	
66	WN3	WN3				WN3b	n	3	32	corr	58	0	..	0.0	..	0.84	
69	WN4	WN4				WN4o	n	3	27	corr	32	0	..	0.2	1.0	0.63	
71	WN7	..				WN7h		2	14		18	1.1	1.2	0.2	0.2	..	
72	B1H+WN3:	CE+WN+B1I	WN6+B1Ia	SB1(WR)	MS86	52	corr	
73	WN4.5+OB	..	WN7,cluster	const RV	Mo89	
75	WN6	WN6		const RV	Mo89	
76	(WN7)	..	WNL/Of	cluster	Mo87,85	
77	(WN+O?)	..	WNL/Of		Mo87	
78	(WN7)	..	WNL/Of		Mo87	
79	WN6	..				WN6o?	n	5	
80	WN7	WN7				WN7h	*	2	21		19	0.8	0.7	0.2	0.1	0.65	
81	WN8	..				WN8o	n	5	
82a	OB+WN5-6:	OB+WN5-6	4-5 WR **	SB,cluster	Mo89,85	WN5o?+OB	*	5	33	corr	..	0	>10	0.0	0.0	..	
82c	WN6		Mo89	WN7?o+OB	*	5	
83	(WN6)	..	WC5	cluster	Mo87	
84	(WN+OB)	..				WN5o	n	5	
85	WN4p	WN3-4p				WN4b		3,4	52	corr	80	0	7.1	0.5	4.0	0.94	
86	WN/Of?	..	WNL/Of	SB1	Mo87,89	
87a1	WN4+WC5?	WN6	WC5	cluster	Mo87	..	*	
87a2	WN6+O	SB1	Mo89	
87b	WN6		Mo87	
88	WN4+OB	WN4.5+a		const RV?	Mo95	WN5+B?	*,n	3	31	corr	4	1.1	
89	WN7	WN6		const RV	Mo89	WN6h	n	1,2,3	18		11	1	1.7	0.3	0.5	0.86	
90	WN7	WN6		SB1	Mo89	WN6(h)	n	1,2,3	17		9	0.4	2.0	0.3	0.7	0.64	
91	WN9 -10:	..		const RV	Mo89	WN9h		2	5		0.6	..	0.1	0.0	0.0	..	
92	WN6	WN6		const RV	Mo89	WN5(h)		2	21		15	0.4	7.5	0.4	2.7	1.04	
95	WN4+OB	WN4+abs				
96	WN3	..				WN4b	*,n	3	31	corr	..	0	10	0.4	1.0	..	
97	WN4+OB	
98	WN4	
99	WN4	WN4				WN4b		3	31	corr	49	0	6.7	0.4	2.5	0.83	
100	WN3-4	WN4		const RV?	Mo95	WN4b		3	34	corr	65	0	5.3	0.5	3.0	0.80	

Notes to Table 7

Column [1]: numbers are direct from Breysacher (1981); letters are subcomponents of a compact cluster as named by Melnick (1985).

Column [5]: binary status: As for Table 6, column [6].

RV Radial velocity

Columns [2], [3] and [6]: references to other classifications and binary status.

Br81	Breysacher (1981)	Me78	Melnick (1978)	Mo89	Moffat (1989)	NS94	Niemela et al. (1994b)
CLP	Conti et al. (1983)	No85	Moffat et al. (1985)	Mo95	Moffat (in preparation)	Wa77	Walborn (1977)
CM89	Conti & Massey (1989)						

Notes to Table 7 — *continued*

Column [8]: notes to the spectra.

n Spectrum affected by nebular emission.

* Notes to individual spectra:

3 Borderline WN3. Triangular profiles.

4 On the TM88 spectrum: 4861 is very weak compared to 4541 and 5411, and appears to be affected by superposed undisplaced absorption. 5875 also shows undisplaced absorption. Effects are possibly due to nebular subtraction.

6 6 and 16 were classed WN2.5 by CM89 on the basis of 'no 4057'. Presence of 5808 indicates lower ionization – WN4.

16 See 6 regarding class. Pickering profiles show central reversal, possibly due to superposed absorption. Lines are also weak for width; see Fig. 16 and Table 8. The differences between the TM88 and Crowther spectra are startling.

21 C iv 5808 ~ He ii 5411 on TM88 spectrum indicates WN5 rather than WN3. N v, iii 4604–40 emission appears to be affected by N iii and C iii absorption. There is a plateau of emission longward of He ii 4686 – also on Br 34; unidentified and unusual.

25 Classification from CM89 data: He i 5875 not present and $FWHM$ 4686 = 31 (corrected).

26 H i 3835 absorption is present on our spectrum.

27 WN3 on basis of weak He i and C iv. However, strong 4100 (N iii + He ii) suggests presence of N iii and hence borderline WN4.

30 Strength of C iv 5808 indicates WN4 not WN3.

33 Heavily affected by O absorption spectrum (and nebular subtraction?). Strong C iv suggests WN5.

34 See 21.

44a AB18 (Azzopardi & Bresacher 1985).

48 Balmer absorption strong and undisplaced; due to a companion and/or nebular subtraction?

51 As for Br 27.

56 All emission lines weak. Absorption superposed on H i 4100, 4340 and probably 4861. Strong nebular emission. N iv 4057 strong.

57 Superposed Balmer absorption clearly visible on Crowther's spectrum.

60 Peculiar. He ii emission lines weak and very narrow for a WN3. He o and C iv absent? If H is really absent, this is the weakest and narrowest line star in this category.

80 R135. In the 30 Doradus nebula.

82 R136. Central cluster of 30 Dor. Melnick spectrum of 'a' is WN5 from the N lines; 'c' is tentatively WN7 from the strength of He i 4471.

87 R140. Moffat et al. (1987) suggest the WC component is a separate star because the C lines are much broader than the N lines.

88 Strong Balmer absorption lines, no helium absorption lines.

96 5800 region is noisy but C iv 5808 is probably present.

Column [9]: source of spectrum used for new classification.

1 From new spectrum, this paper, resolution 4–6 Å.

2 Crowther, private communication, resolution 2–3 Å.

3 Our inspection of TM88 spectrum; $FWHM$ and EW 5411 from CM89, resolution 10–156 Å.

4 Koesterke et al. (1991); 5411 and 5808–75 regions only, resolution 1–2 Å.

5 Melnick (1985), resolution 3.5 Å.

Column [10]: notes to $FWHM$ 4686.

5411 $FWHM$ 5411 from Koesterke et al. (1991).

corr $FWHM$ 4686 is taken from CM89 or direct from TM88 spectrum and corrected for an instrumental resolution of 12 Å; see Section 5.

a wider range of application. Therefore the two plots which give best overall discrimination between ionization subclasses are N iv/N v, iii and C iv/He i versus He ii/He i. These are shown in Figs 9 and 10 for Galactic WN stars.

Fig. 9 is the plot of N iv/N v, iii against He ii/He i for Galactic WN stars. It displays the separation of subclass by the He ionization – except for WN5, which straddles WN4 and WN6, and is marked by strong N iv/N v, iii. Values for WN3 stars are too uncertain to plot, but the limits (+1, –1 dex) place them off the diagram in the lower right corner.

Stars which present themselves as unusual in this diagram are the following.

(1) The WN7/C stars fall below the others of their subclass due to presence of carbon in the 4640-Å blend.

(2) The values plotted for the Carina 'ha' stars WR 22, 24 and 25 are from the high-resolution spectra of Crowther et al. (1995b); the present classification system does not manage these stars well (see Section 3.4).

(3) The WN5–6b stars WR 36 and 110 are discussed in

Section 4. Despite a N v/N iii ratio which places them in the WN5 subclass, WR 36 has He ii/He i on the border with WN7, and both have N iv 4057 weaker than normal for a narrow-line WN5 star.

(4) WR 1 and 37 have a He ii/He i ratio which is within observational uncertainty of the WN4/6 boundary, but on the WN6 side; the ratio of N v/N iii > 2 makes them WN4, rather than WN6.

Fig. 10 is the plot of C iv/He i against He ii/He i for Galactic WN stars. Both ratios are extremely ionization-sensitive and correlate well. The boundaries are those given in Table 4(a) defining the ionization subclasses. Separation is good but not perfect. The WN/C stars fall high due to strong C iv 5808. WR 43 is the cluster NGC 3603, containing three WR stars (see Moffat, Seggewiss & Shara 1985; Moffat, Drissen & Shara 1994; Moffat et al. 1996, in preparation), and the values are uncertain because the lines are weak.

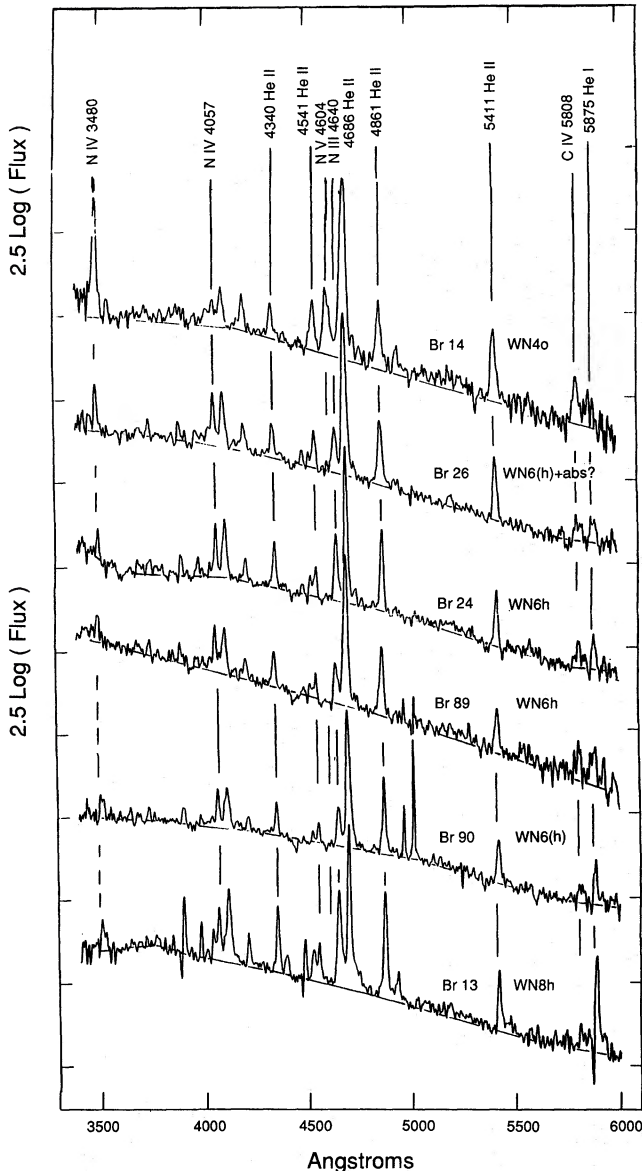


Figure 8. Our limited sample of LMC WN spectra.

6.2 He/N ratio – the effects of abundance

Fig. 11 plots the EW ratio $\text{He II } 4686/\text{N V,III } 4604-40$ against Galactocentric radius $R(\text{Gal})$ from VdH88. Distances of stars will change slightly as a result of reclassifications. However, since recalibration of the M_p is also in order, and because no quantitative conclusions are drawn from this diagram, the VdH88 values of $R(\text{Gal})$ serve our purpose.

The He/N ratio depends on both ionization subclass and on $R(\text{Gal})$. For WN5–8 stars, the ratio increases to earlier subtype and to larger $R(\text{Gal})$. The averages for LMC stars are plotted at $R(\text{Gal}) = 15$ kpc and are close to the extrapolations of the Galactic relationships for these subclasses.

The change with $R(\text{Gal})$ presumably reflects the local Z values, which ultimately determine the nitrogen abundance in the WN atmosphere. The difference in line ratio between

the LMC and the solar neighbourhood is about a factor of 2, somewhat less than the factor 3–4 for average Z . The average gradient in Fig. 11 (assuming He-abundance is constant) is $d \log N/dR = -0.04 \text{ dex kpc}^{-1}$; this is lower than the accepted value for the Galactic disc, $-0.1 \text{ dex kpc}^{-1}$ (Hron 1989), and the mean value of $-0.08 \text{ dex kpc}^{-1}$ observed in H II gas in a number of external spiral galaxies (Belley & Roy 1992). The presence of the gradient is consistent with the theoretical prediction that nitrogen abundance in WN stars reflects the initial (C+N+O) abundance of the progenitor star. More detailed abundance analyses by Crowther et al. (1995a) show a similar effect with Galactic position; however, those by Smith & Willis (1983) and Crowther et al. (1995b) do not.

The four Galactic WN3 stars scatter from nearly the highest ratio (WR 127) to nearly the lowest ratio (WR 3). WN4 stars are mostly above the WN5 stars, but show no dependence on $R(\text{Gal})$.

6.3 N IV 3480/4057

CM89 remark on the different behaviour of these two N IV lines. Fig. 12 shows the ratio of the lines, based on the peak line/continuum measure and our data only. The strength of the triplet 3480 relative to the singlet 4057 increases to earlier subtype, and increases with increasing strength of both lines.

7 LINE STRENGTH AND WIDTH, IONIZATION SUBCLASS, AND HYDROGEN ABUNDANCE

Figs 13–17 displays EW 5411 versus $FWHM$ 4686, with various subgroups highlighted.

7.1 Binaries and $\text{H}^+/\text{He}^{++}$

Fig. 13 shows strength versus width for the Galactic WN stars, with distinctive symbols for binary and composite stars (crosses) and stars displaying hydrogen (filled squares). Note the following points.

(1) The single stars follow a well-defined, but non-linear relationship. The correlation was previously noted by Bohannan (1990).

(2) The known spectroscopic and spectrum binaries (including composite stars) have lines that are too weak for their width. The strength–width relationship for single stars is sufficiently well defined that the line weakening can be used to estimate the continuum contribution by the companion (see Section 7.2 and Table 8).

(3) The transition to $FWHM$ 4686 $> 30 \text{ \AA}$ and EW 5411 $> 40 \text{ \AA}$ is nearly simultaneous. HKW include WR 91 as ‘s’. WR 46 and some binaries are ‘b’ but not ‘s’ only because of EW reduction by the companion. WR 46 is an SB1 WN3b star with a 7-h period (van Genderen et al. 1991; Niemela et al. 1995a). Its position suggests strongly that the companion contributes to the continuum even if no absorption lines are visible.

(4) Stars with hydrogen detected fall at the weak-narrow end of the relationship. The limits for hydrogen presence are approximately $FWHM$ 4686 $< 30 \text{ \AA}$ and EW 5411 $< 25 \text{ \AA}$

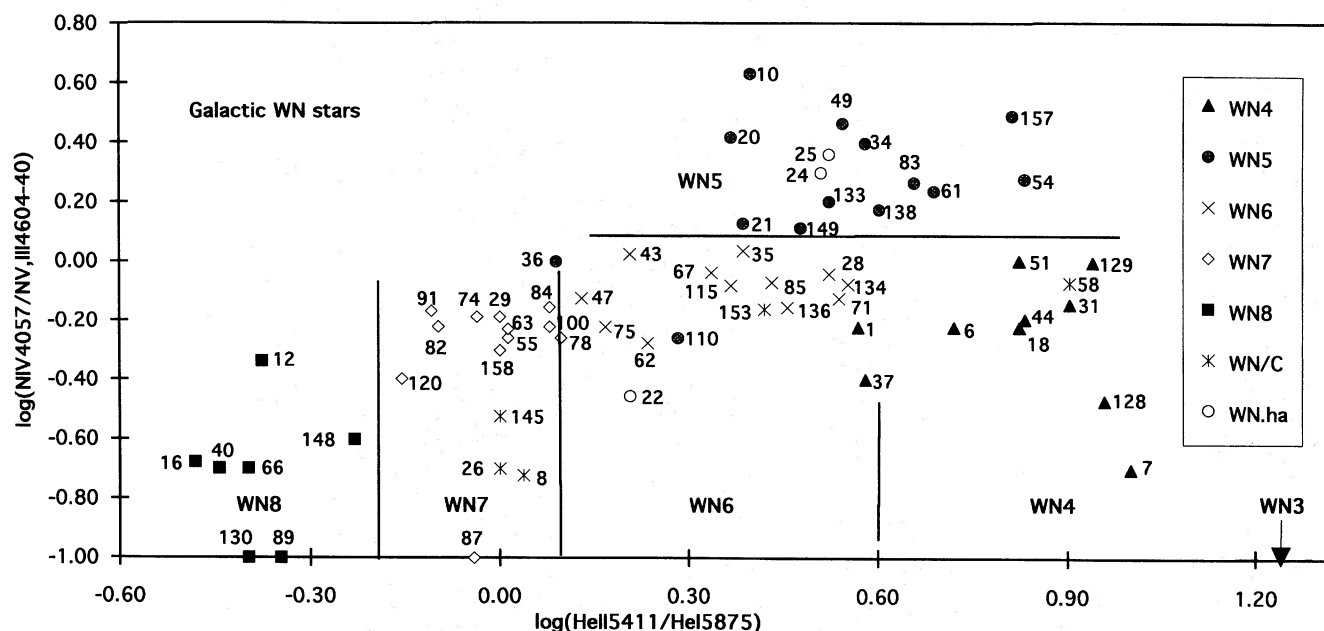


Figure 9. The plot of $\log(\text{N iv } 4057/\text{N v, III } 4604-40)$ against $\log(\text{He II } 5411/\text{He I } 5875)$, using the peak/continuum measure for the line strengths, for Galactic WN stars (see Table 6). The boundaries are those given in Table 4a defining the ionization subclasses. Values for WN3 stars are too uncertain to plot, but the limits ($+1$, -1 dex) place them off the diagram in the lower right corner. Stars mentioned in the text are identified with VdH81 numbers.

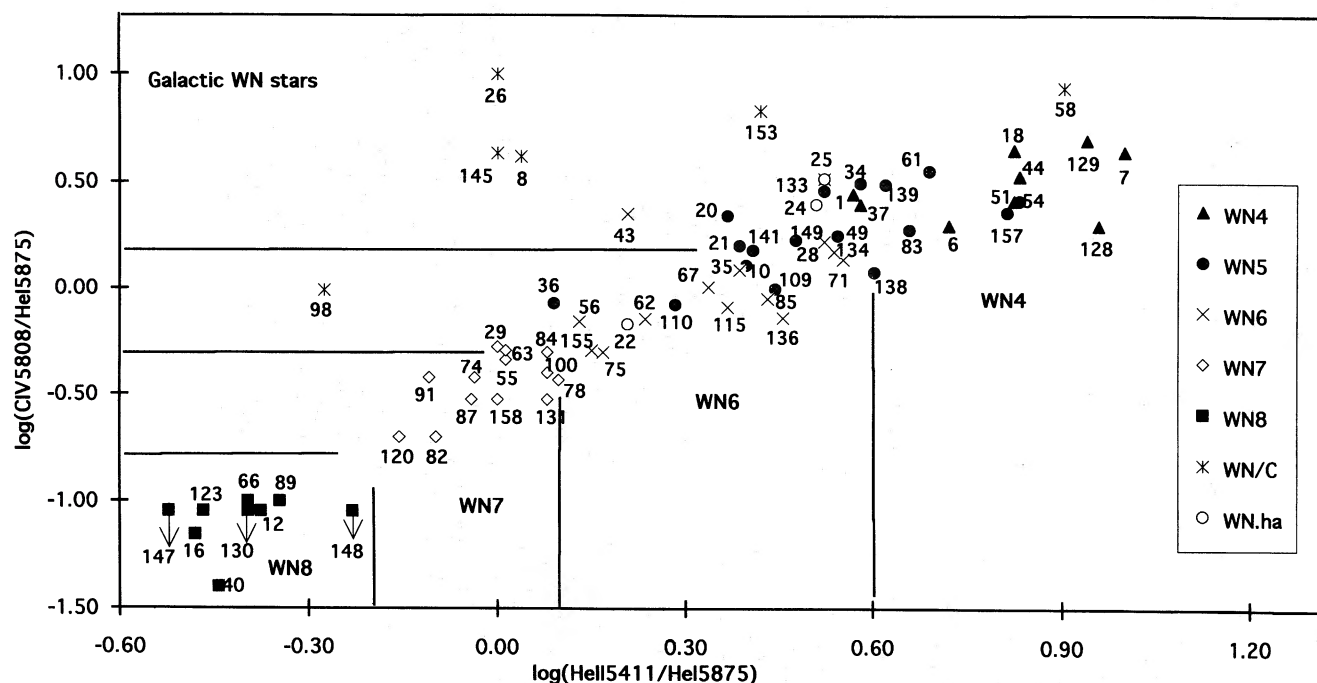


Figure 10. The plot of $\log(C\text{ iv }5808/\text{He\text{ i }5875})$ against $\log(\text{He\text{ ii }5411}/\text{He\text{ i }5875})$, using the peak/continuum measure for the line strengths, for Galactic WN stars (see Table 6). The boundaries are those given in Table 4(a) defining the ionization subclasses. Stars mentioned in the text are identified by the VdH81 numbers.

with small overlap both ways. The overlap (see below) mostly disappears when the ionization subclasses are separated. WR 136 is an outrageous exception to the norm (see Section 10).

(5) A few stars fall wild and deserve comment. WR 2 is the only WN2 star in the Galaxy. *EW* 5411 is significantly

less than for other broad-line stars, but is comparable to BR 4 (the WN2 star in the LMC). WR 91 and 100 are WN7b stars; the line widths are dramatically greater than for other WN7 stars. WR 7 (WN4b) and WR 149 (WN50) have emission lines which are unusually narrow for their strength but the spectra are otherwise quite normal.

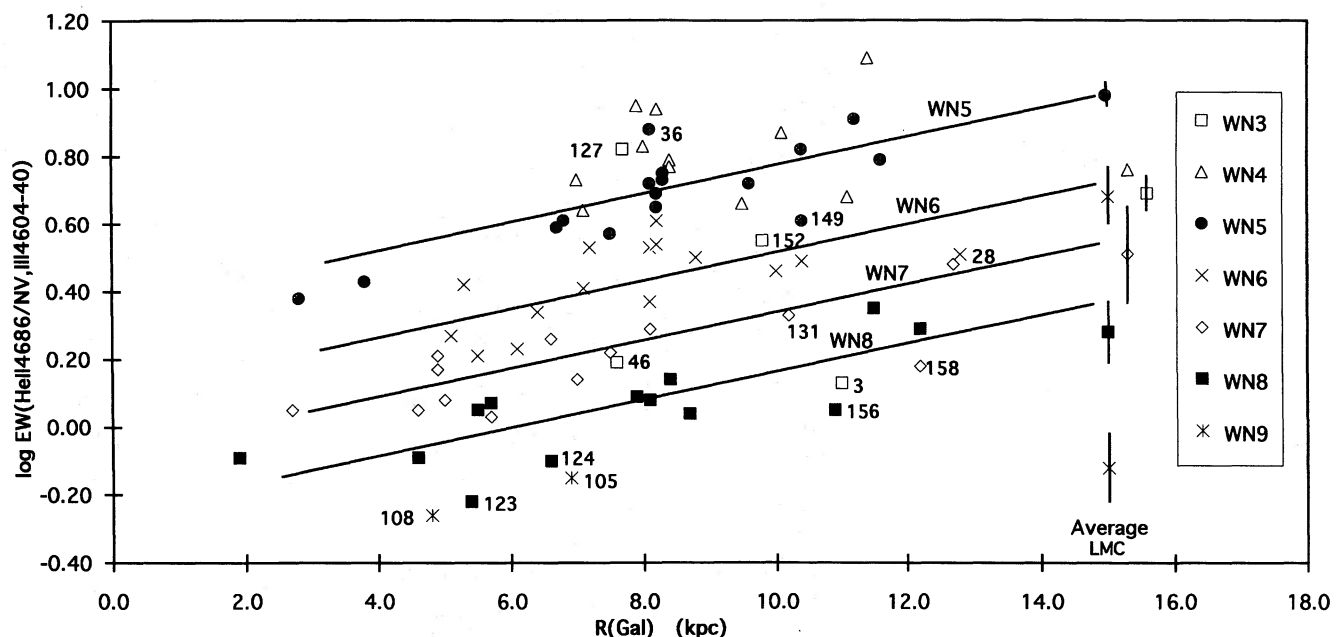


Figure 11. The plot of the EW ratio $\log(\text{He II } 4686/\text{N V, III } 4604-40)$ against Galactocentric radius from VdH88. The slope of the lines is approximately $d \log(N_{\text{III}})/dR = -0.04 \text{ dex kpc}^{-1}$. The average for LMC str is plotted at a Galactocentric radius of 15 kpc with error bars of \pm one standard error of the mean. Stars mentioned in the text are identified by the VdH81 numbers.

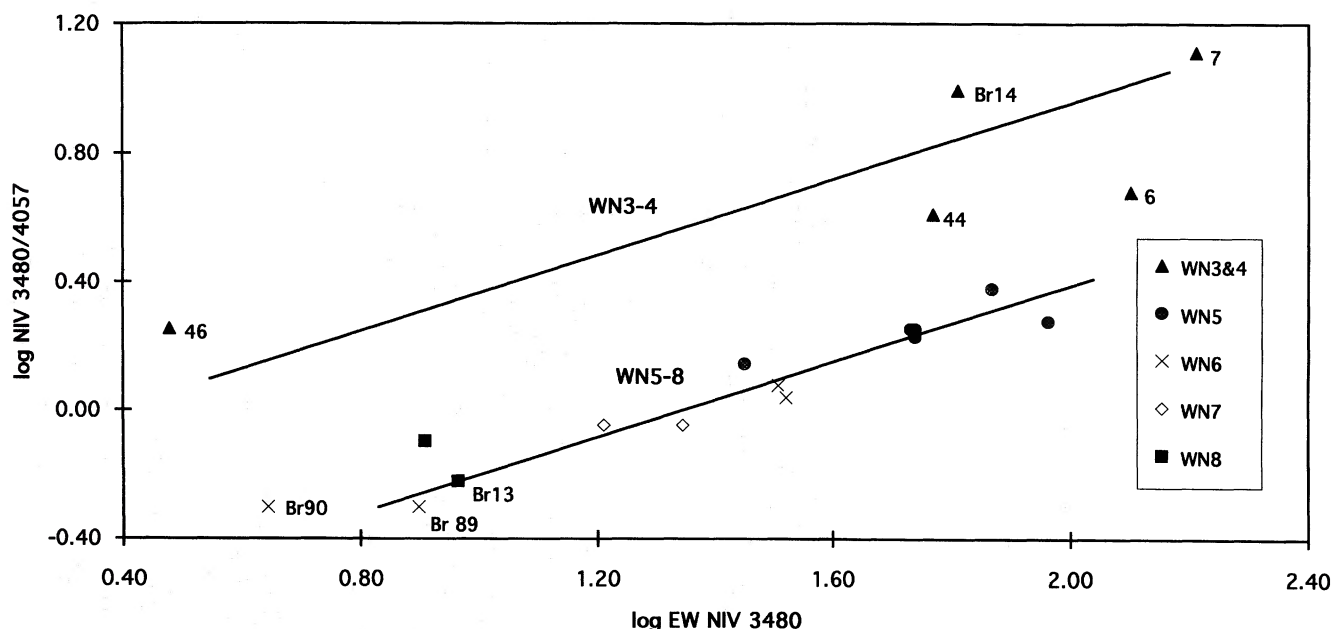


Figure 12. The plot of $\log(N_{\text{IV}} 3480/4057)$, using the peak/continuum measure for the line strengths and our data only (Table 3). The strength of the triplet 3480 relative to the singlet 4057 increases to earlier subtype and increases with the increasing strength of both lines. Stars with extreme values and LMC stars are identified with the VdH81 and Br81 numbers.

Fig. 14 is the same as Fig. 13, but for the WN stars in the LMC. Most of the same comments apply.

- (1) The relationship defined by single stars is the same as for the Galaxy.
- (2) The binary and composite spectra stars are well separated from the single stars.
- (3) The transition to $FWHM 4686 > 30 \text{ \AA}$ and EW

$5411 > 40 \text{ \AA}$ is nearly simultaneous. Only Br 3, 20, 23 and 35 have strong lines, but $FWHM 4686 > 30$ (corrected CM89 values).

(4) Stars with hydrogen detected fall at the weak-narrow end of the relationship. The limits for hydrogen presence are about the same as for the Galactic WN stars. Unfortunately, the hydrogen content of Br 80 is unknown. There is again one outrageous exception. BR 60 has weak, narrow

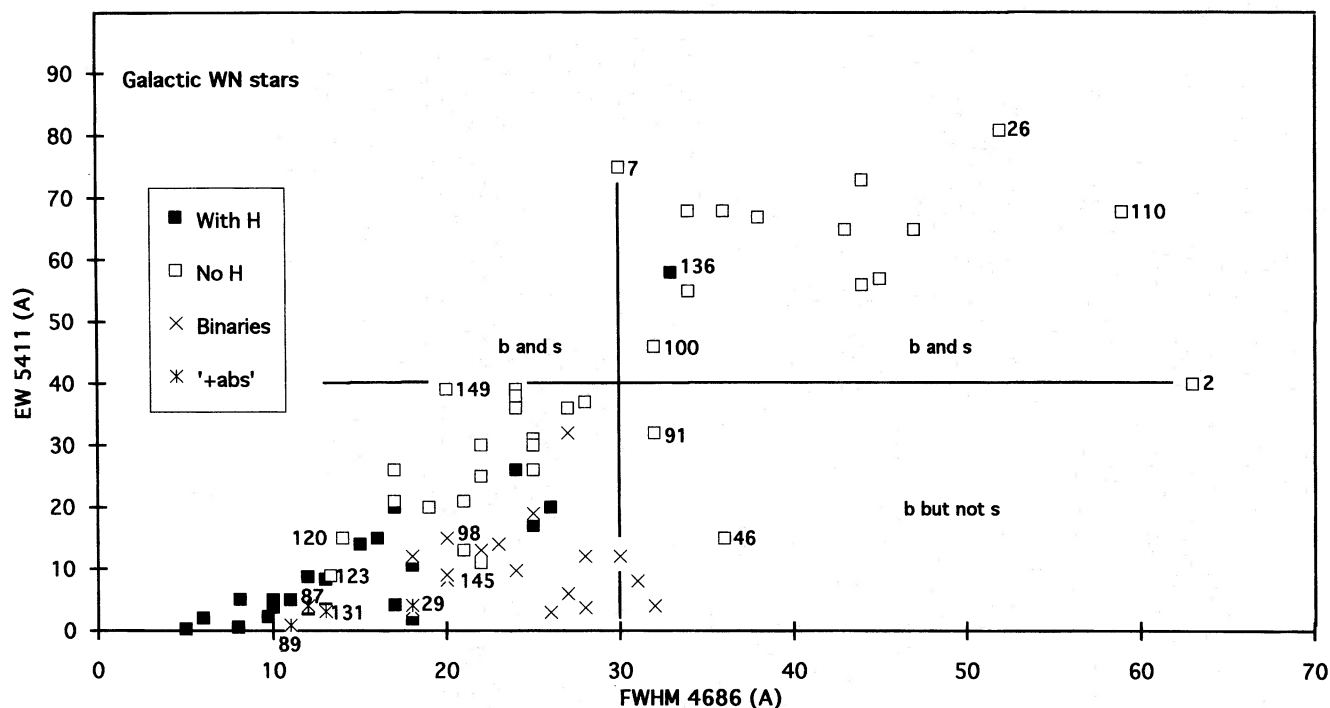


Figure 13. The plot of $EW\ 5411$ versus $FWHM\ 4686$ for Galactic WN stars (Table 6) with distinctive symbols for binary and composite stars (crosses) and stars displaying hydrogen (filled squares). The lines give the boundaries of the 'b' stars defined in this paper, and the 's' stars defined by HKW. Stars mentioned in the text are identified with VdH81 numbers.

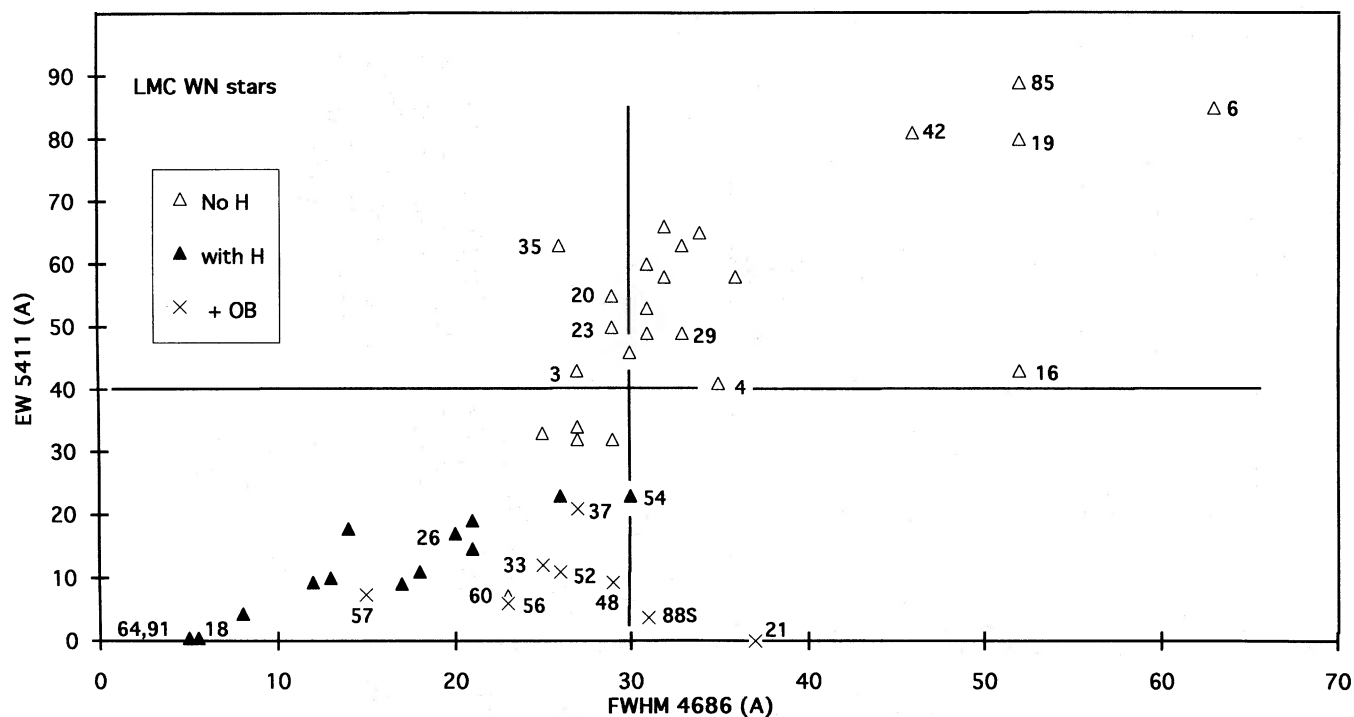


Figure 14. The plot of $EW\ 5411$ versus $FWHM\ 4686$ for LMC WN stars (Table 7) with distinctive symbols for binary and composite stars (crosses) and stars displaying hydrogen (filled triangles). The lines give the boundaries of the 'b' stars (see Fig. 12). Stars mentioned in the text are identified with Br81 numbers.

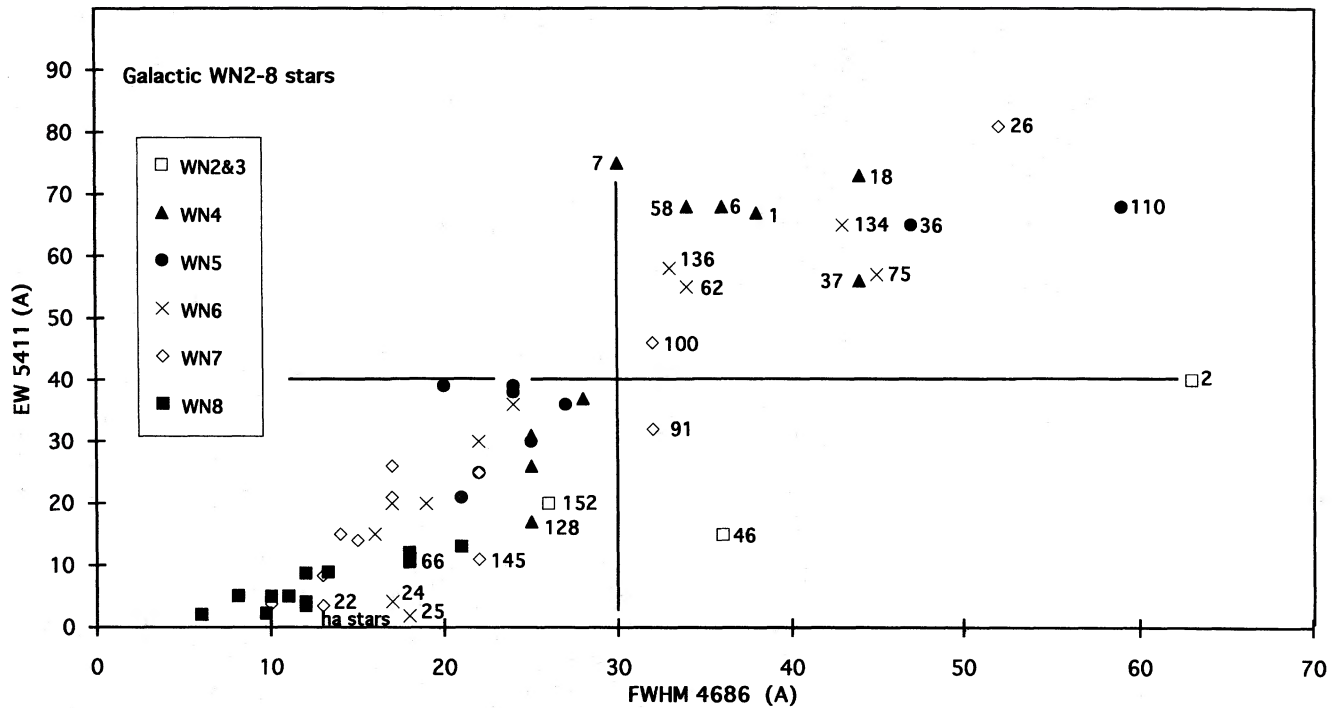


Figure 15. The plot of $EW\ 5411$ versus $FWHM\ 4686$ for Galactic WN stars (Table 6). The binaries are omitted, and the points are coded by ionization subclass. Stars mentioned in the text are identified with VdH81 numbers.

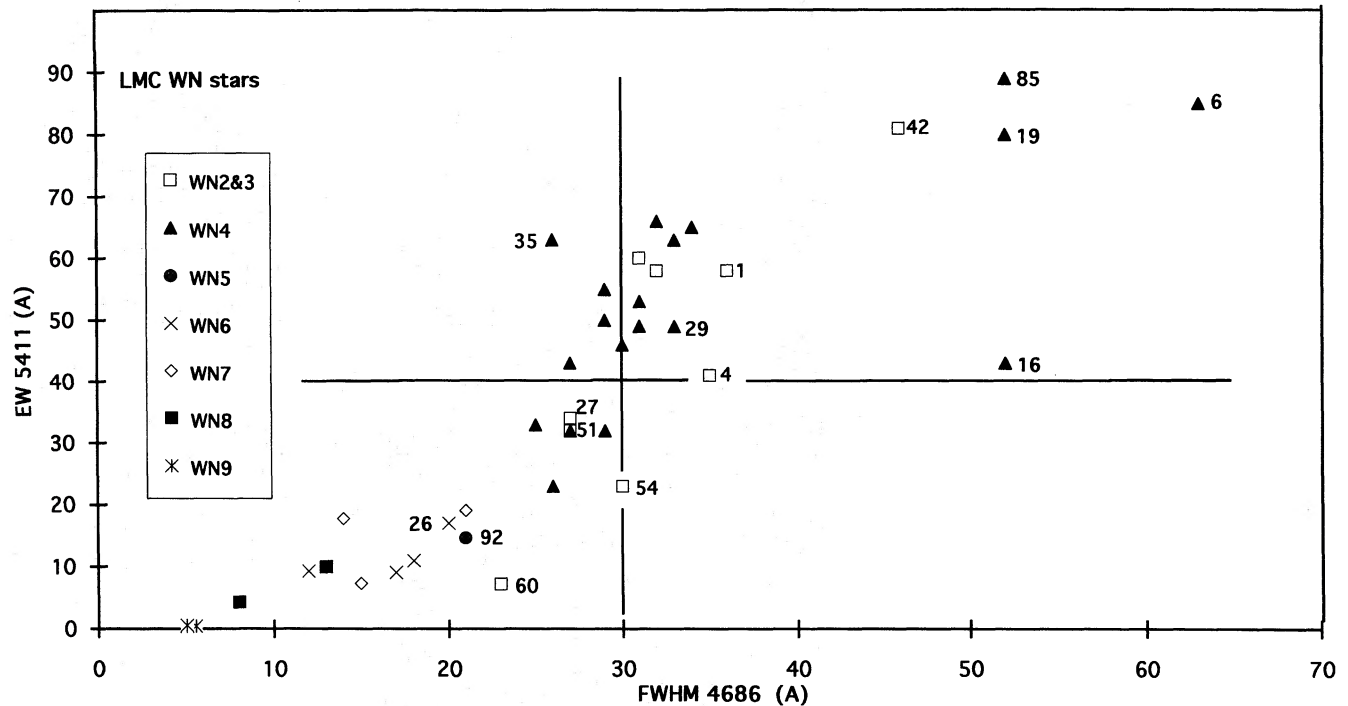


Figure 16. The plot of $EW\ 5411$ versus $FWHM\ 4686$ for LMC WN stars (Table 7). The binaries are omitted, and the points are coded by ionization subclass. Stars mentioned in the text are identified with Br81 numbers.

lines and no detected hydrogen. The TM88 spectrum we inspected is noisy; confirmation is needed.

(5) Br 4 (WN2b) and 16 (WN4b) have very weak (H I + He II) 4861 compared to He II 5411 and 4541. Superposition of broad absorption seems the most likely explanation.

They are retained in future diagrams but are perpetually numbered.

Table 8 gives observed and expected EWs for composite stars (for which we have EW and FWHM measurements in

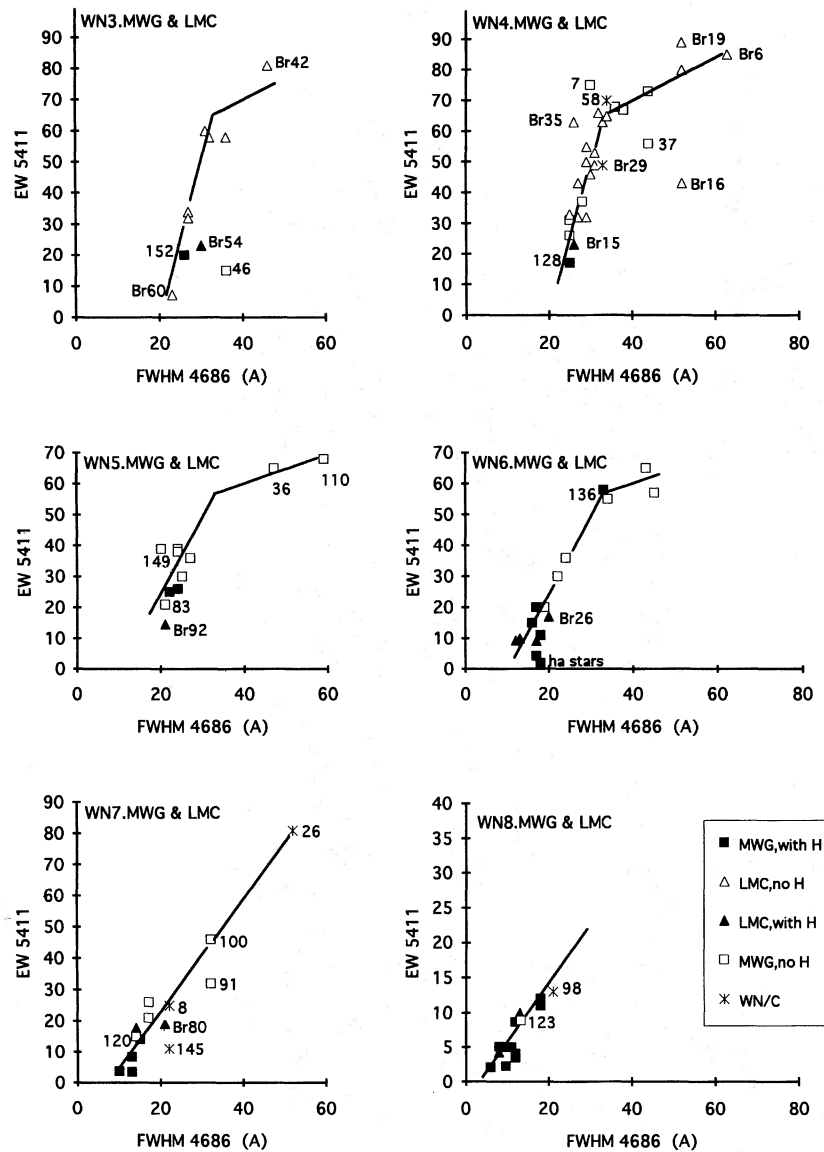


Figure 17. The plots of $EW\ 5411$ versus $FWHM\ 4686$ for Galactic and LMC WN stars (Tables 6 and 7) for each ionization subclass. Galactic and LMC stars are distinguished by squares (Galaxy) and triangles (LMC). Stars with hydrogen detected are plotted as filled symbols. Stars with strong carbon are plotted as * (both Galactic and LMC) and are numbered. Binaries are omitted. The lines are drawn by eye for the purpose of defining the expected EW for a given FWHM. The equations are given in Table 8. If WR 36 and 110 (classified WN5–6b; see Section 4) were plotted with the WN6 rather than with the WN5, the WN5 stars could be equally well fitted by the WN3–4 relationship.

Tables 5 and 6), together with the relative luminosity at 5411 of an OB companion which would account for the difference. Stars WR 46, 91 and 145, Br 4 and 16 are included, despite the absence of a clear OB signature in the spectrum, because they fall well below the expected relationships for single stars. Also included are the ‘+ abs’ stars WR 29, 87, 89 and 131, which may prove to be ‘ha’ stars.

7.2 Ionization subclass, H^+/He^{++} and WN/C stars

Figs 15 and 16 are again the EW versus FWHM diagrams for the Galaxy and LMC, respectively. The binaries are omitted, and the points are coded by ionization subclass. The ‘+ abs’ stars are also omitted; they fall in the domain occupied by the ‘ha’ stars. There are similarities between the

two galaxies. The WN8 stars occupy the low end, and earlier subclasses occupy domains increasingly far to the high end of the strength–width relation. The ionization subclasses are only partially separated; there is considerable overlap. Differences are more interesting. In the Galaxy, the transition zone from narrow- to broad-line stars, $FWHM \sim 30\ \text{\AA}$ and EW between 40 and 50 \AA , is almost empty. In the LMC, this part of the diagram is filled with WN4 stars.

Fig. 17 plots the EW–FWHM diagram for each ionization subclass with Galactic and LMC stars together but distinguished by squares (Galaxy) and triangles (LMC). Stars with hydrogen detected are plotted as filled symbols. Stars with strong carbon are plotted as * (both Galactic and LMC) and are numbered. Binaries are omitted. The lines in Fig. 17 are drawn by eye for the purpose of defining the

Table 8. Estimates of relative brightness of companion stars based on the observed and the expected equivalent width of He II 5411.

WR #	Spectrum	Binary status	FWHM 4686 (Å)	EW 5411 (Å)		OB/WR	Luminosity +/- [1]
				Observed	Expected		
3	WN3b + O4	SB1?	31	8	55	6	4
10	WN5h (+ OB)	visual	20	8.2	25	2	2
21	WN5o + O4-6	SB2	27	6	43	6	4
29	WN7h + abs	...	18	4.1	19	4	3
31	WN4o + O8V	SB2	28	12	40	2	1
43	WN6o (+ O5)	cluster	26	3	40	12	8
46	WN3b pec	SB1	36	15	67 [2]	3	1
47	WN6o + O5V	SB2	23	14	33	1.4	0.6
63	WN7o + OB	...	18	12	19	0.6	0.4
87	WN7h + abs	...	12	4	8.6	1.2	1.3
89	WN8 + abs	...	11	0.9	6.3	6.0	4.2
91	WN7b	...	32	32	45	0.4	0.4
97	WN5b + O7	SB2	32	4	55	13	8
127	WN3b + O9.5V	SB2	30	12	50	3	1
131	WN7h + abs	...	13	3.1	10.5	2	2
133	WN5o + O9I	SB2	28	3.7	45	11	7
138	WN5o + B7	SB2	22	13	30	1.3	0.6
139	WN5o + O6	SB2	24	9.7	35	3	1
141	WN5o + OB	SB2	27	32	43	0.3	0.4
145	WN7o/CE + OB?	SB1	22	11	27	1.5	0.7
151	WN4o + O5V	SB2	25	19	25	0.3	0.4
153	WN6o/CE + O6I	SB2,quad	20	9	25	2	2
155	WN6o + O9II/b	SB2	18	3.4	20	5	3
157	WN5o (+ B1I)	visual	20	15	25	0.7	0.5
Br #							
4	WN2b + OB?	...	35	41	70 [2]	1	..
16	WN4b + OB?	...	52	43	78	0.8	0.5
21	WN5?b + B1Ia	SB2?	37	0	56	large	..
26	WN6(h) + abs?	SB1	20	17	25	0.5	0.4
33	WN5o + O	...	25	12	37	2	0.8
37	WN4 + OB	SB2	27	21	35	0.7	0.5
48	WN4o? + B	const RV?	29	11	43	3	1
52	WN4h + abs	const RV?	26	11	30	1.7	0.8
56	WN5o? + OB	...	23	6	33	5	3
57	WN7h + OB	...	15	7.4	14	1	1
88	WN5 + B7	const RV?	31	3.7	53	13	8

Relationships used for calculation of expected EW for single stars - Figure 16.
FWHM < 33 FWHM > 33

WN3-4	EW = 5.0 FWHM - 100	EW = 0.7 FWHM + 42
WN5-6	EW = 2.5 FWHM - 25	EW = 0.45 FWHM + 42
WN7	EW = 1.8 FWHM - 13	
WN8	EW = 0.85 FWHM - 3	

Relationships used for calculation of expected EW for single stars (Fig. 16).

	FWHM > 33	FWHM > 33
WN3-4	EW = 5.0 FWHM - 100	EW = 0.7 FWHM + 42
WN5-6	EW = 2.5 FWHM - 25	EW = 0.45 FWHM + 42
WN7	EW = 1.8 FWHM - 13	
WN8	EW = 0.85 FWHM - 3	

- [1] Uncertainties are estimated individually on the basis of: ± 0.1 or 0.2 dex in EW according as the EW 5411 is $>$ or $< 10 \text{ \AA}$ (see Table 9); and $\pm 1 \text{ \AA}$ in $FWHM$. No allowance is made for the uncertainty in the formulae used to calculate the expected value of EW 5411.
- [2] The EW predictions for WR46 (WN3bpec) and Br 4 (WN2) are based on the assumption that the WN3-4 relationship is valid.

expected EW for a given $FWHM$. The equations are given in Table 8. If WR 36 and 110 (classified WN5-6b, see Section 4) were plotted with the WN6 rather than the WN5, the WN5 stars could be equally well fitted by the WN3-4 relationship.

Notable features of Fig. 17 are as follows.

(1) The EW - $FWHM$ relationships are extremely well defined. Much of the scatter in Figs 13-16 is due to differences between ionization subclasses. There are a few exceptions. Br 6 and 16 (WN4b) are the previous WN2.5 stars (CM89) with exceptionally broad lines. Br 16 and WR 46 (WN3b, SB1) are suspected composite spectra, discussed above. WR 145 (WN7o/CE) is an SB1 (Massey & Grove 1989), and its line strength suggests that the companion makes a significant contribution to the continuum; $H\beta$ has structure suggesting the presence of strong superposed absorption.

(2) The Carina WN6ha and WN7ha stars fall neatly on the lower ends of their sequences, with ultraweak and narrow lines.

(3) The WN/C stars are amongst the strongest and widest line spectra in their respective subclasses. The exception is WR 153 (WN6o/CE + O6I), which has narrow lines ($FWHM$ 4686 = 20 \AA); it is not in the diagram because it is a binary.

(4) Stars with hydrogen are the weakest and narrowest line stars in each subclass. The exceptions are WR 136 [WN6b(h)], with marginal hydrogen and broad-strong lines, and two weak-narrow-line stars, Br 60 (WN3o) and WR 83 (WN5o), which show no hydrogen on TM88 spectra. These deserve further investigation.

(5) The generalization (Smith & Willis 1983) that LMC stars have stronger He lines than corresponding Galactic stars is confirmed for WN3 and WN4 stars, but not for later subclasses.

Note that, despite the general trend of increasing line width towards earlier subtypes, we define the b-stars by an absolute value for $FWHM$ rather than relative to an average for the subclass for three reasons: (1) to keep the definition of the three dimensions independent; (2) because of the limit of 30 \AA seems to correspond to a significant change in the physical properties of the star (see HKW); and (3) because the meaning of 'average' is poorly defined (see Section 7.3).

The boundary above which hydrogen is *not* found is a function of ionization subclass; the division is cleaner in EW than in $FWHM$ (see Fig. 17). We find the boundaries at (width, strength) = (30, 25) for WN3-5 and (20, 20) for WN6-7. The boundary for WN 8 is not well defined. There is no evidence at this time for a difference between the two galaxies.

For stars *with* hydrogen, both $FWHM$ 4686 and EW 5411 correlate with the H^+/He^{++} ratio. Fig. 18 gives the plot of $\log EW$ 5411 versus H^+/He^{++} .

7.3 Differences between the Galaxy and the LMC

The frequency distributions of WN stars among the ionization subclasses is shown in Fig. 19; it is dramatically different in the Galaxy and the LMC. The Galactic distribution rises to WN5 and remains high for later subclasses; the LMC distribution peaks very sharply at WN4. Stars without classification on the present criteria are plotted separately, based on subclasses given by Breysacher (1981). Variations within the Galaxy also occur (see, e.g., Smith 1968b and

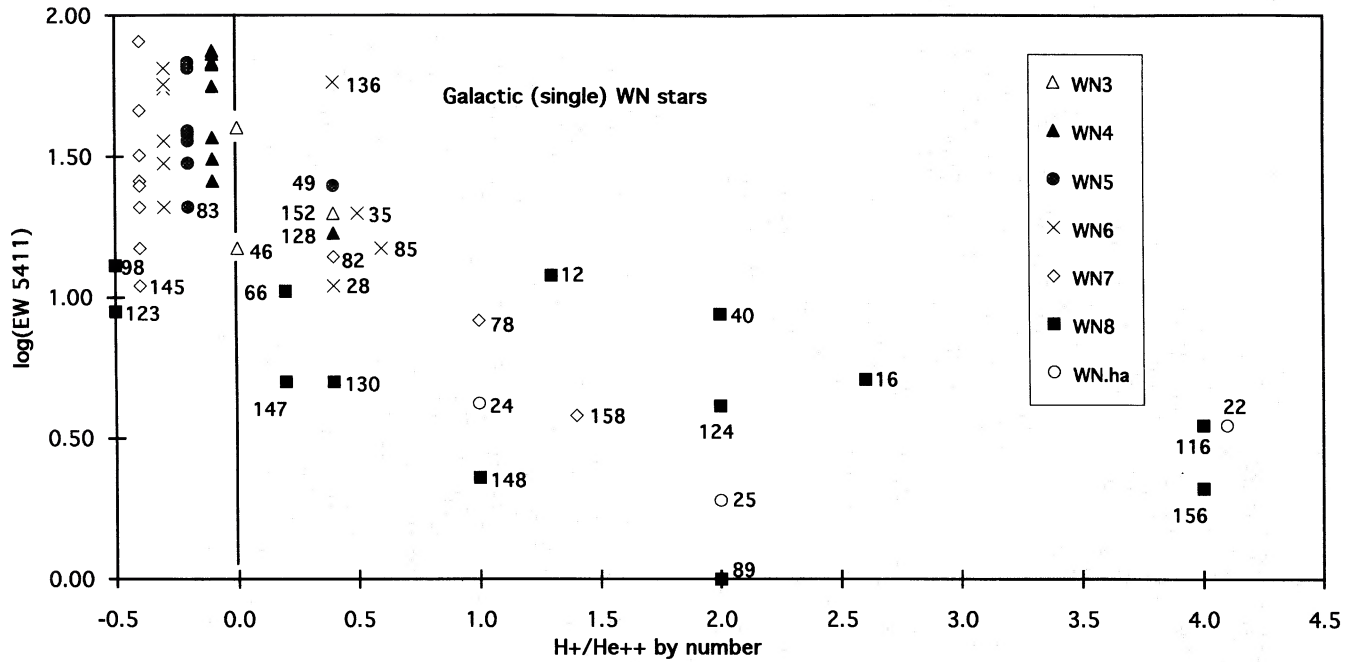


Figure 18. The plot of $\log(EW\ 5411)$ versus H^+/He^{++} (by number) for single, Galactic WN stars (Table 6). Zero values of H^+/He^{++} are spread over 0.0 to -0.5 to improve visibility.

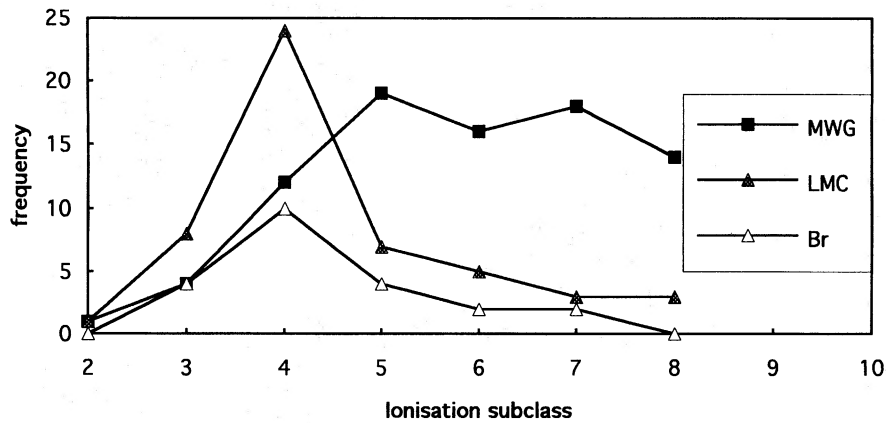


Figure 19. The frequency distributions of WN stars in the Galaxy (Table 6) and the LMC (Table 7) among the ionization subclasses. Stars without classification on the present criteria are plotted separately, based on subclasses given by Br 81.

VdH88); re-evaluation of these is outside the scope of this paper.

The frequency distribution in the EW–FWHM diagram are also different. This may be seen qualitatively by comparing Figs 15 and 16. In the Galaxy, there is a gap between the narrow- and broad-line stars; in the LMC the WN4 stars fill that gap.

Fig. 20 shows the frequency distributions in $FWHM\ 4686$ for all stars in Tables 5 and 6 (single and composite) with available data (LMC data are incomplete). The distributions for the WN4 and WN5 stars are different, with the maximum frequencies in the LMC occurring for broader lines. The differences are statistically significant, with chi-squared probabilities of 4×10^{-6} and 0.02, respectively.

The frequency distribution of stars with or without detected hydrogen are similar for WN2–5 stars. However,

there is, as yet, no known LMC WN6–8 star without hydrogen, compared to 50 per cent of Galactic WN6–8 stars in this category.

8 CONFUSION IN THE OLD SYSTEM CLASSIFICATION

The reasons for the inadequacy of the old system of classification are now reasonably clear.

(1) The overall visual appearance of the spectrum between 4000 and 5000 Å is dominated by the line width, and by the strength of the N III and N V lines relative to He II 4686. These parameters *correlate* with ionization subclass; however, ranges overlap and these parameters do not *discriminate* between subclasses.

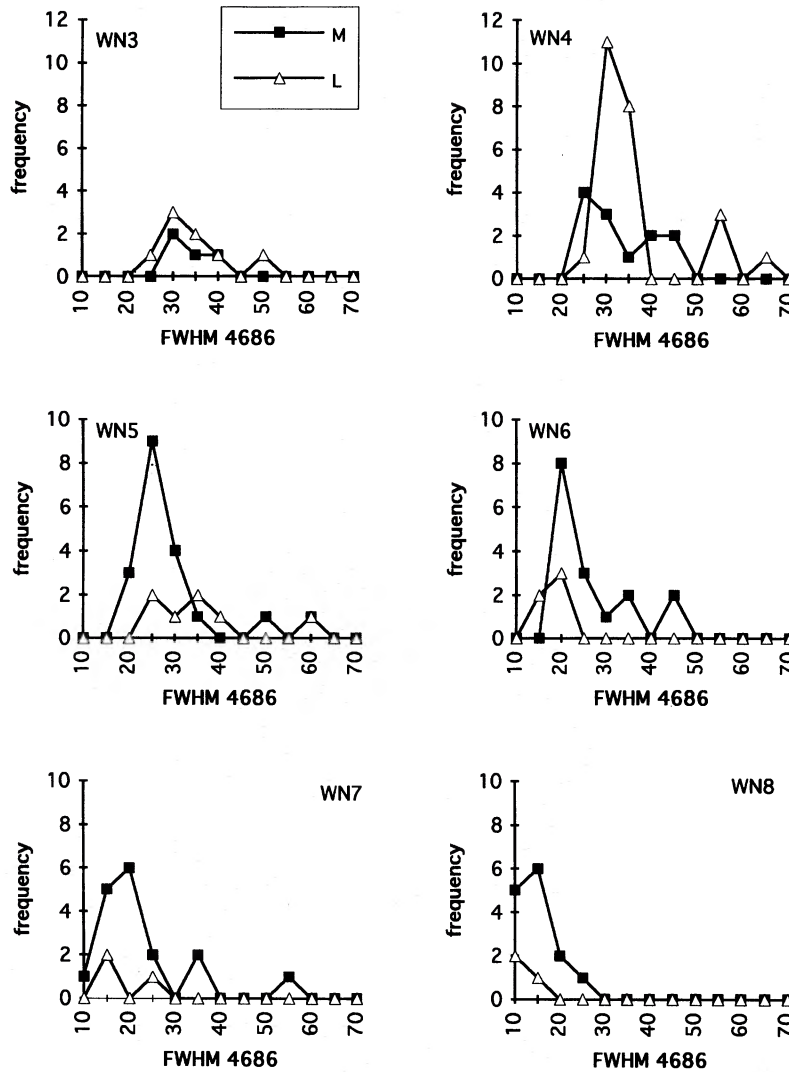


Figure 20. The frequency distributions in *FWHM 4686* for all stars in Tables 5 and 6 (single and composite) with available data (LMC data are incomplete).

(2) Confusion is compounded by the proximity of critical lines – so that line width and spectral resolution of the observation can dramatically affect the appearance.

(3) The N/He ratio is affected by abundance as well as ionization.

As a specific example, HD 50896 was chosen as the standard star for WN5. It is now WN4b. This is not a result of incorporating the subclass 4.5 as a full digit; it reflects a fundamental confusion. The objective definition of WN5 was $N_{III} \approx N_{IV} \approx N_V$. On any modern wavelength-calibrated spectrum (and, in fact, already in the Atlas), it is clear that HD 50896 has strong, broad N_V with weak if any N_{III} in the gap between N_V and He II 4686. Without an objective wavelength scale, the eye tends to judge the distance between the lines by comparison to the linewidth; when there is little or no gap, the wavelength difference is judged smaller and the broad N_V 4604 is attributed, in part, to N_{III} 4640. A further confusion arises from the choice of HD 50896 as the standard star of WN5: because classifica-

tion is done by comparison of spectra, not just objective criteria, line strength and width have become unofficial classification criteria.

9 ACCURACY AND VARIABILITY

Table 9 compared EW measures of 4686, 5411 and 4604–40 from CLP, CM89, the Smith & Kuhl Atlas (1981) and the present paper. CLP and Atlas values are derived from photographic spectra; CM89 and the present data are from linear detectors. We have good agreement with CM89. CLP values are systematically lower with strong lines being more affected than weak lines.

The EW ratios, $EW(H_{\alpha} \text{ 4686}/N_{V,III} \text{ 4604–40})$ given in the present paper and CM89 agree well. However, for $EW(He \text{ II } 5411/He \text{ I } 5875)$ the agreement is poor. We suspect lower accuracy of the He I 5875 measures due to the interstellar lines, blending with C IV 5808 (in b-stars) and often low signal-to-noise ratio in the continuum.

Table 9. Accuracy of observations.

log EW	Authors compared		EW range	n	Average	St.Dev.
5411	HKW	/ CM89	All	41	-0.01	0.11
			EW > 10 Å	28	-0.02	0.08
			EW < 10 Å	9	0.01	0.19
	This paper	/ CM89		21	0.04	0.07
4686	CLP	/ CM89	All	52	-0.18	0.15
			EW > 100 Å	24	-0.21	0.15
			EW < 100 Å	28	-0.16	0.15
	Atlas	/ CM89		9	-0.05	0.05
	This paper	/ CM89		27	0.05	0.07
4604-40	CLP	/ CM89		48	-0.14	0.17
	Atlas	/ CM89		8	-0.10	0.10
	This paper	/ CM89		23	0.04	0.09
log (EW1/EW2)	Authors compared			n	Average	St.Dev.
4686 / 4604-40	This paper	/ CM89		20	-0.01	0.06
5411 / 5875	HKW	/ CM89		28	0.06	0.10
	This paper	/ CM89		17	0.14	0.15
	This paper	/ HKW		18	0.06	0.11

With the improvement in accuracy that results from linear detectors, it becomes reasonable to identify stars with EW measures differing by more than 2σ as probably variable. The most obvious case is WR 36 (WN5-6b), with EW 4686 from CM89 being per 60 per cent of ours and the line narrower (43 Å compared to our 47 Å). In Table 6, WR 46 (WN3b pec) is also flagged as variable on the basis of the report by van Genderen et al. (1991) of phase-dependent variations of 10–25 per cent in the EW.

Measured line width is affected by resolution. Spectra of CM89/Us/Crowther have resolutions of 10–15/4–6/2–3 Å, respectively. For *FWHM* below 30 Å, differences between observers are generally as expected from the resolution. For *FWHM* > 30 Å (b-stars), resolution should have little effect; however, the differences between observers are often larger than expected from observational uncertainty alone. In addition to WR 36, discussed above, we flag WR 6 and 8 as probably variable, and WR 18, 43 and 110 as possibly variable. For all WN3 stars, *FWHM* from different observers are discordant; however, the profiles are triangular rather than Gaussian, and the measured width depends on how the half-maximum is defined.

10 EVOLUTION

Evolutionary considerations indicate (e.g., Maeder & Meynet 1994) that WN stars evolve to decreasing H abundance and suddenly increasing C and O abundances as they convert to WC stars. Fig. 17 shows that, within each ionization subclass, stars with H show the weakest and narrowest lines, and stars with enhanced C are among the strongest and broadest lined objects. *This indicates that evolution in the WN phase is marked by steadily increasing line strength and width, i.e., WN stars evolve from 'ha' to 'h' to '(h)' to 'o' to 'b' to 'C'.*

Combinations 'b(h)' or 'h/C' are not expected. WR 136 [WN6b(h)] was found by HKW, and confirmed by Crowther & Smith (1995), to have a small amount of hydrogen, below

the level of reliable detection by the Pickering decrement method. Presence of hydrogen in this star is a startling exception to all general trends. There is no case of a WN/C star with hydrogen.

Ionization subclasses WN3–8 include stars with some hydrogen at the narrow-line end and no hydrogen at the broad-line end. In the Galaxy, the percentage showing hydrogen in each subclass increases smoothly from 12 per cent for WN2–4 to about 80 per cent for WN8. In the LMC, numbers are roughly the same for WN2–5, but all WN6–8 stars appears to have hydrogen. All WN9 stars so far investigated have hydrogen.

Crowther et al. (1995c,d) have made a good case for evolution through WN9 and 10 and LBV to WN7h and WN8h with decreasing H abundance. The next question is whether a star *continues* to evolve to earlier subclass or not.

As emphasized by Meynet et al. (1994) and by Crowther et al. (1995d), the high- and low-mass progenitors must be considered separately. Very high-mass stars suffer so much mass loss, both on and immediately after the main sequence, that the core shrinks leaving a thick envelope with H/He decreasing smoothly towards the centre. These stars can remain WN most of their lives, evolving to lower mass, lower luminosity and lower hydrogen abundance. The very young clusters, such as 30 Dor and Carina, are dominated by WN6h(a) and WN7h(a), but the greater 30 Dor region also contains WN8o (Br 81), WN6o (Br 79), WN5o (Br 82a), WN4o (Br 69) and WN3b (Br 66) stars. *It would appear that the massive star scenario encompasses all ionization subclasses of WN but mostly in the narrow-line form.*

For the lower mass stars, the initial change in mass and bolometric luminosity of the models during the WN phase is small, corresponding to removal of a shallow He–N shell. M_{e} , mass and ionization subclass are well correlated (Lundstrom & Stenholm 1984c; VdH88; Smith & Maeder 1989; Moffat 1981, 1982, 1995). HKW find that the 's' stars are much hotter than the 'w' stars. It follows that, as the star

evolves from an 'o' to a 'b' star, its temperature increases and, assuming a corresponding increase in the bolometric correction, the visual luminosities will become fainter. It therefore appears inevitable that, *as a star evolves from 'h' to 'o' to 'b', it must move to earlier subtype*. The WN ionization subclass(es) through which a star passes will be determined by its mass when it arrives at the WN phase.

The proportion of stars with hydrogen decreases to earlier subclass. This is consistent with the assertion above that later stages of the WN lifetime will manifest as an earlier subclass.

11 CONCLUSIONS

The WN stars are a rather more complex group than the WC stars. WC star models can be defined by two parameters, present mass and C/He ratio (neglecting O/C as of secondary importance); the structure is simple and does not depend on the previous history. To define a WN star requires present mass, N/He and H/He and structural data. The thickness of the H/He/N shell is probably important, and that depends on the history of the star: initial mass, mass-loss rate, binary or not, metallicity. It is therefore not surprising that the classification system needed to describe WN spectra is somewhat more complex than for WC spectra. However, the one proposed here manages to sort the stars into groups which are closely similar in appearance and which show smooth and systematic trends of properties. Some of the properties of the subclasses have direct interpretation into the evolutionary scheme.

WN stars in the LMC can be classified by the criteria established in the Galaxy with no conflicts arising. There are differences between the Galaxy and LMC in the frequency distributions of stars over: ionization subclass; EW and FWHM for WN4 and 5; and probably H content for WN6–8. These differences are presumably due to the difference in the primordial heavy-element abundance. How Z affects the subclasses of WN is still unexplained.

ACKNOWLEDGMENTS

LFS thanks the Director's Discretionary Research Fund at the Space Telescope Science Institute for support while the paper was being written. AFJM is grateful for financial assistance to NSERC (Canada) and FCAR (Quebec). MMS gratefully acknowledges support from NASA via grant NAGW-2913. All three authors thank Mike Potter for help at the telescope and in data reduction, and Paul Crowther for providing copies of spectra and data therefrom prior to publication, and for extensive discussions.

REFERENCES

- Annuk K., 1991, in van der Hucht K. A., Hidayat B., eds, Proc. IAU Symp., Wolf-Rayet Stars and Interrelations with other Massive Stars in Galaxies. Reidel, Dordrecht, p. 245
- Antokhin I. I., Betrand J.-F., Lamontagne R., Moffat A. F. J., Matthews J. M., 1995, AJ, 109, 817
- Azzopardi M., Breysacher J., 1985, A&A, 149, 213
- Beals C. S., 1938, Trans. IAU, 6, 248
- Belley J., Roy J.-R., 1992, ApJS, 78, 61
- Bohannan B., 1990, in Garmany C. D., ed., ASP Conf. Ser. Vol. 7, Properties of Hot Luminous Stars. Astron. Soc. Pac., San Francisco, p. 39
- Breysacher J., 1981, A&AS, 43, 203
- Castor J. I., van Blerkom D., 1970, ApJ, 161, 485
- Conti P. S., Massey P., 1989, ApJ, 337, 251 (CM89)
- Conti P. S., Leep E. M., Perry D. N., 1983, ApJ, 268, 228 (CLP)
- Conti P. S., Massey P., Vreux J.-M., 1990, ApJ, 354, 359
- Crowther P. A., 1993, PhD thesis, Univ. London
- Crowther P. A., Smith L. J., 1996, A&AS, 305, 541
- Crowther P. A., Hillier D. J., Smith L. J., 1995a, A&A, 293, 172
- Crowther P. A., Hillier D. J., Smith L. J., 1995b, A&A, 293, 403
- Crowther P. A., Smith L. J., Hillier D. J., Schmutz W., 1995c, A&A, 293, 427
- Crowther P. A., Smith L. J., Hillier D. J., 1995d, in van der Hucht K. A., Williams P., eds, Proc. IAU Symp. 163, Wolf-Rayet Stars: Binaries, Colliding Winds, Evolution. Reidel, Dordrecht, p. 147
- Crowther P. A., Smith L. J., Willis A. J., Hillier D. J., van der Hucht K. A., Williams P., eds, Proc. IAU Symp. 163, Wolf-Rayet Stars: Binaries, Colliding Winds, Evolution. Reidel, Dordrecht, p. 152
- Grandchamp A., Moffat A. F. J., 1991, in van der Hucht K. A., Hidayat B., eds, Proc. IAU Symp. 143, Wolf-Rayet Stars and Interrelations with other Massive Stars in Galaxies. Reidel, Dordrecht, p. 258
- Hamann W.-R., Koesterke L., Wessolowski U., 1993, A&A, 274, 397 (HKW)
- Hamann W.-R., Koesterke L., Wessolowski U., 1995, A&AS, 113, 459
- Havlen R. J., Moffat A. F. J., 1977, A&A, 58, 351
- Hillier D. J., 1987, ApJS, 63, 965
- Hiltner W. A., Schild R. E., 1966, ApJ, 143, 770 (HS66)
- Hron J., 1989, A&A, 222, 85
- Isserstedt J., Moffat A. F. J., Niemela V. S., 1983, A&A, 126, 183
- Koenigsberger G. Firmani C., Bisiacchi G. F., 1980, Rev. Mex. Astron. Astrofis., 5, 45
- Koesterke L., Hamann W.-R., Schmutz W., Wessolowski U., 1991, A&A, 248, 166
- Lamontagne R., Moffat A. F. J., Seggewiss W., 1983, ApJ, 269, 596
- Lewis D., Moffat A. F. J., Matthews J. M., Robert C., Marchenko S. V., 1993, ApJ, 405, 312
- Lundstrom I., Stenholm B., 1984a, A&A, 138, 311
- Lundstrom I., Stenholm B., 1984b, A&AS, 56, 43
- Lundstrom I., Stenholm B., 1984c, A&AS, 58, 163
- Maeder A., Meynet G., 1994, A&A, 287, 803
- Marchenko S., Moffat A. F. J., Koenigsberger G., 1994, ApJ, 422, 810
- Massey P., 1981, ApJ, 244, 157
- Massey P., Grove K., 1989, ApJ, 344, 870
- McCandliss S. R., Bohannan B., Robert C., Moffat A. F. J., 1994, Ap&SS, 221, 155
- Melnick J., 1978, A&AS, 34, 383
- Melnick J., 1985, A&A, 153, 235
- Meynet G., Maeder A., Schaller G., Schaerer D., Charbonnel C., 1994, A&AS, 103, 97
- Moffat A. F. J., 1981, in Chiosi C., Stalio R., eds, Proc. IAU Colloq. 59, Effects on Mass Loss of Stellar Evolution. Reidel, Dordrecht, p. 301
- Moffat A. F. J., 1982, in de Loore C. W. H., Willis A. J., eds, Proc. IAU Symp. 99, Wolf-Rayet Stars: Observations, Physics, Evolution. Reidel, Dordrecht, p. 515
- Moffat A. F. J., 1989, ApJ, 347, 373
- Moffat A. F. J., 1992, A&A, 253, 425
- Moffat A. F. J., 1995, in van der Hucht K. A., Williams P., eds, Proc. IAU Symp. 163, Wolf-Rayet Stars: Binaries, Colliding Winds, Evolution. Reidel, Dordrecht, p. 213
- Moffat A. F. J., Niemela V. S., 1984, ApJ, 284, 631

- Moffat A. F. J., Seggewiss W., 1978, *A&A*, 70, 69
Moffat A. F. J., Lamontagne R., Seggewiss W., 1982, *A&A*, 114, 135
Moffat A. F. J., Seggewiss W., Shara M. M., 1985, *ApJ*, 295, 109
Moffat A. F. J., Lamontagne R., Shara M. M., McAlister H. A., 1986, *AJ*, 91, 1392
Moffat A. F. J., Niemela V. S., Phillips M. M., Chu Y.-H., Seggewiss W., 1987, *ApJ*, 312, 612
Moffat A. F. J., Drissen L., Shara M. M., 1994, *ApJ*, 436, 183
Niemela V. S., 1980, in Plavec M. J., Popper D. M., Ulrick R. K., eds, *Proc. IAU Symp. 88, Close Binaries: Observations and Interpretation*. Reidel, Dordrecht, p. 177
Niemela V. S., 1982, in de Loore C. W. H., Willis A. J., eds, *Proc. IAU Symp. 99, Wolf-Rayet Stars: Observations, Physics, Evolution*. Reidel, Dordrecht, p. 299
Niemela V. S., 1991, in van der Hucht K. A., Hidayat B., eds, *Proc. IAU Symp. 143, Wolf-Rayet Stars and Interrelations with other Massive Stars in Galaxies*. Reidel, Dordrecht, p. 201
Niemela V. S., 1995, in van der Hucht K. A., Williams P., eds, *Proc. IAU Symp. 163, Wolf-Rayet Stars: Binaries, Colliding Winds, Evolution*. Reidel, Dordrecht, p. 223
Niemela V. S., Moffat A. F. J., 1982, *ApJ*, 259, 213
Niemela V. S., Conti P. S., Massey P., 1980, *ApJ*, 241, 1050
Niemela V. S., Mandrini C. H., Mendez R. H., 1985, *Rev. Mex. Astron. Astrofis.*, 11, 143
Niemela V. S., Barb'a R., Shara M. M., 1995a, in van der Hucht K. A., Williams P., eds, *Proc. IAU Symp. 163, Wolf-Rayet Stars: Binaries, Colliding Winds, Evolution*. Reidel, Dordrecht, p. 245
Niemela V. S., Seggewiss W., Moffat A. F. J., 1995b, in van der Hucht K. A., Williams P., eds, *Proc. IAU Symp. 163, Wolf-Rayet Stars: Binaries, Colliding Winds, Evolution*. Reidel, Dordrecht, p. 251
Robert C. et al., 1992, *ApJ*, 397, 277
Schmutz W., Hamann W.-R., Wessolowski U., 1989, *A&A*, 210, 236
Smith L. F., 1968a, *MNRAS*, 138, 109
Smith L. F., 1968b, *MNRAS*, 141, 317
Smith L. F., 1973, in Bappu M. K. V., Sahade J., eds, *Proc. IAU Symp. 49, Wolf-Rayet and High Temperature Stars*. Reidel, Dordrecht, p. 15
Smith L. F., Kuhi L. V., 1981, *JILA Report No. 117*. Univ. Colorado, Boulder
Smith L. F., Maeder A., 1989, *A&A*, 211, 71
Smith L. J., Willis A. J., 1983, *A&AS*, 54, 229
Smith L. F., Shara M. M., Moffat A. F. J., 1990a, *ApJ*, 348, 471
Smith L. F., Shara M. M., Moffat A. F. J., 1990b, *ApJ*, 358, 229
Smith L. F., Shara M. M., Moffat A. F. J., 1995, in van der Hucht K. A., Williams P., eds, *Proc. IAU Symp. 163, Wolf-Rayet Stars: Binaries, Colliding Winds, Evolution*. Reidel, Dordrecht, p. 48
Torres-Dodgen A. V., Massey P., 1988, *AJ*, 96, 1076 (TM88)
Underhill A. B., Hill G. M., 1994, *ApJ*, 432, 770
van der Hucht K. A., Conti P. S., Lundstrom I., Stenholm B., 1981, *Space Sci. Rev.*, 28, 227
van der Hucht K. A., Hidayat B., Admiranto A. G., Supelli K. R., Doom C., 1988, *A&A*, 199, 217 (VdH88)
van Genderen A. M. et al., 1991, in van der Hucht K. A., Hidayat B., eds, *Proc. IAU Symp. 143, Wolf-Rayet Stars and Interrelations with other Massive Stars in Galaxies*. Reidel, Dordrecht, p. 129
Walborn N. R., 1974, *ApJ*, 189, 269
Walborn N. R., 1977, *ApJ*, 215, 53
Willis A. J., Stickland D. J., 1990, *A&A*, 232, 89